Research Square

Preprints are preliminary reports that have not undergone peer review.
They should not be considered conclusive, used to inform clinical practice,
or referenced by the media as validated information.

Assessment of Various Biochemical Indicators and Gene Markers Regulating Plant Physiology and Biochemistry Under Fluoride Toxicity

Adarsh Pratap Singh
Jawaharlal Nehru University
Ananya Singh
Jawaharlal Nehru University
Shekhar Mallick
shekharm@mail.jnu.ac.in

Jawaharlal Nehru University

Research Article

Keywords: Fluoride Phytotoxicity, F− transporters, Biochemical Indicators, Mitigation Strategies

Posted Date: November 20th, 2026

DOI: https://doi.org/10.21203/rs.3.rs-11577297/v1

License: This work is licensed under a Creative Commons Attribution 4.0 International License.
Read Full License

Additional Declarations: No competing interests reported.

Assessment of Various Biochemical Indicators and Gene Markers Regulating Plant Physiology and Biochemistry Under Fluoride Toxicity

Adarsh Pratap Singh[a], Ananya Singh[a], Shekhar Mallick[*a]
a: School of Environmental Science, Jawaharlal Nehru University, New-Delhi-110067
*: Corresponding author: Shekhar Mallick, Professor,
email: shekharm@mail.jnu.ac.in

Abstract:

Fluoride (F^-) is recognized as a persistent and potent phytotoxicant, widely distributed in the Earth's crust (0.06-0.09%) and gradually mobilized through anthropogenic activities such as phosphate fertilizer (SSP & DAP) application and aluminum smelting. Unlike other halides, F^-'s high electronegativity permits it to accumulate within plant tissues, primarily through stomatal uptake or root absorption, leading to profound physiological perturbations. This review synthesizes a comprehensive understanding regarding the mechanisms of F^- uptake through various F^- transporters and the toxicity disrupting the fundamental biochemistry of plant systems.

At the cellular level, F^- stress induces a cascade of metabolic dysfunctions. It significantly impairs the synthesis and stability of essential molecules, including structural proteins and fatty acids, leading to membrane lipid peroxidation and altered fluidity. Photosynthetic efficiency is often compromised due to the degradation of chlorophyll pigments and the inhibition of Rubisco activity. Furthermore, F-stress alters the profile of amino acids and secondary metabolites, often triggering an overproduction of proline and polyphenols as a defensive response. The various reported F^- transporters in plants viz. FEX, ABC transporters, ALMT, CLC, NRT/NPF, and their mechanism is reviewed and a generalized view have been proposed mostly from *Camelia sinensis* and *Arabidopsis thaliana*.

The review also highlights the proposed mechanism of transport of F^- across the various reported transporters and the knowledge gap for future research.

Keywords: Fluoride Phytotoxicity, F^- transporters, Biochemical Indicators, Mitigation Strategies.

1.0 *Introduction : General chemistry and geogenic occurrence of* F^-

Fluorine (F), the 13th most abundant element in the Earth's crust, accounts for approximately 0.059% of its mass, with an average concentration of ~557 mg kg^{-1} in the continental crust and considerably higher concentrations in certain F-rich granitic and metamorphic rocks (Ghosh et al., 2013; Rudnick & Gao, 2014; Vithanage and Bhattacharya, 2015). Owing to its exceptionally high electronegativity (3.98 on the Pauling scale) and strong chemical reactivity, fluorine rarely occurs in its elemental form in nature and is predominantly present in the −1 oxidation state as fluoride (F^-) in minerals and other compounds (Takeda et al., 2008). Elemental fluorine exists as diatomic F_2 gas under ambient conditions and reacts readily with numerous elements, including certain noble gases such as xenon. In aqueous environments, F^- may occur as free F^- or form complexes with metal cations, whereas its protonated form, hydrofluoric acid (HF; pKa ≈ 3.2), becomes increasingly relevant under acidic conditions (Johnston and Strobel, 2020).

Environmental F^- originates from both geogenic and anthropogenic sources. Geogenic inputs primarily arise from the weathering and dissolution of F^--bearing minerals, including fluorite (CaF_2), fluorapatite [$Ca_5(PO_4)_3F$], cryolite (Na_3AlF_6), villiaumite (NaF), topaz, and F^--containing silicate minerals such as micas and amphiboles, commonly associated with granites, pegmatites, and syenites (Saxena and Ahmed, 2003; Vithanage et al., 2015). Anthropogenic contributions are largely associated with coal combustion, Al smelting, and the manufacture and application of phosphate fertilizers, including diammonium phosphate, monoammonium phosphate, single superphosphate, and nitrogen–phosphorus–potassium formulations (Li et al., 2023). Fluoride concentrations in coal vary considerably depending on geological origin, while Al production can release F^--containing gaseous and particulate emissions into the atmosphere, contributing to environmental contamination (Tjahyono et al., 2011; Singh et al., 2018).

The combined influence of natural geochemical processes and anthropogenic activities contributes to elevated F- concentrations in groundwater, making F^- contamination a major environmental and public health concern, with more than 200 million people worldwide estimated to be exposed to elevated levels (Vithanage et al., 2015). The World Health Organization (WHO) recommends a guideline value of 1.5 mg L^{-1} for F^- in drinking water. Reported groundwater F^- concentrations vary widely across geographical regions, ranging from approximately 0.01 to 48 mg L^{-1} globally. In South Asia, concentrations of approximately 0.01–10 mg L^{-1} have been reported, with localized hotspots reaching 15–16 mg L^{-1} (Emamjomeh and Sivakumar, 2009; Vithanage et al., 2015). Prolonged exposure to excessive F^-, particularly through contaminated drinking water, can result in dental and skeletal fluorosis and has also been associated with adverse effects on several organ systems, including the kidneys, liver, and endocrine system (Ghosh et al., 2013).

1.1 Soil chemistry of F^-

Soil acts as a primary reservoir for environmental F^-, where most F^- occurs in mineral lattices or adsorbed onto clays and Fe/Al oxy-hydroxides, with only a small fraction present in soil solution. Fluoride accumulates predominantly in upper soil layers because oxides, silicates, and aluminium hydroxides [$Al(OH)_3$] strongly retain it. Upon entering soil, F^- undergoes rapid ion exchange followed by slower precipitation reactions forming fluorite (CaF_2) and fluorapatite ($Ca_5(PO_4)_3F$) (Prabhu et al., 2023). The distribution and mobility of F^- depend on soil physicochemical properties such as pH, cation-exchange capacity (CEC), sorbent mineralogy, and salinity. Fluoride is concentrated mainly in the clay/colloidal fraction and forms soluble or sparingly soluble complexes with Ca^{2+}, Mg^{2+}, Fe^{3+}, and Al^{3+} depending upon the pH; it can also form complexes with silica (SiF_4, SiF_6^{2-}), hydroxide complex with boron ($[BF_n(OH)_{4-n}]^-$), and trace metals including Be, V, Ur and rare-earth elements (Serrano et al., 2000; Sivasankar et al., 2016; Nordstorm and Jenne, 1977). Fluoride occurs largely as free F^- or aquo-complexes in neutral groundwater, and due to the presence of little or no dissolved Fe and Al, the F^- is unable to form complexes with these cations (Edmunds & Smedley, 20; Ozsvath, 2009). Soil pH strongly controls F^- -solubility, where acidic conditions enhance dissolution of metal–F- complexes, and alkaline soils tend to retain soluble F^-; nevertheless, labile F^- from mineral phases can leach to groundwater under diverse pH conditions depending on weathering and soil maturity (Manoharan et al., 2007; Skjelkvåle, 1994; Zhu et al., 2007). The equilibrium activity of F^- in soils is governed by associated mineral activities, particularly Ca^{2+} and Al^{3+} controlling CaF_2 and AlF_3 equilibria (Prabhu et al., 2023). Regulatory guidance such as the Canadian soil quality guideline sets 400 mg kg^{-1} as a threshold for residential/parkland soils (Prabhu et al., 2023). Although anthropogenic activities, such as the application of phosphate fertilizers containing F^- impurity, whereas other sources include coal, steel, Al, Cu, and Ni smelting, glass, fertilizer, brick, and tile industries, contribute significantly in surface soil contamination (Pickering 1985; Skjelkvåle 1994). In contrast, geogenic processes play a significant role in groundwater F^- contamination. The anionic sorption capacity of Fe (hydr)oxides is inversely proportional to pH (point of zero charge is between 8.5 and 9.3) due to the development of negatively charged surfaces at higher pH, resulting in desorption of anions, i.e., As (as AsV) and F^- (Streat et al., 2008). Both these anions are strongly held to the positive surfaces of the Fe (hydr)oxide matrix, which get detached as free ions with increasing pH under reducing conditions. Due to similar desorption patterns of As and F^- from Fe (hydr)oxides with the pH increase, the co-contamination of the above anions in the oxidizing aquifers is quite possible (Bhattacharya et al., 2006; Farooqi et al., 2007; Currell et al., 2011).

1.2 Toxic manifestations of F^- in plants and animals

Fluoride is biologically reactive due to its strong affinity for metal cations such as Ca^{2+}, Mg^{2+}, and Fe^{2+}, forming complexes that disrupt physiological processes including Ca-mediated signaling (Barbier et al., 2010; Johnston and strobel., 2020). In animals, F^- toxicity operates through multiple mechanisms—protein inhibition, organelle damage, altered intracellular pH, and electrolyte imbalance—affecting metabolism at molecular, cellular, and organ levels. F^- is a xenobiotic

inhibitor of essential phosphoryl-transfer enzymes. Fluorine, often in the form of aluminum fluoride (AlF^{-}_{4}) or (AlF_3) or beryllium fluoride (BeF^{-}_{3}) complexes formed with metals like (Mg^{2+}), which acts as a transition-state analogue, hence strongly inhibiting enzymes that catalyze phosphoryl transfer (Berkowitz et al., 2008) (Figure 1 A, B). Because of its high affinity for Al, F^- forms AlF_4^- complexes that mimic phosphate, inhibiting phosphate-dependent enzymes such as ATPases and G-proteins and thereby impairing energy metabolism, signaling, and biosynthesis (Barbier et al., 2010). (Figure1 A).

The key inhibited enzymes thus includes, Enolase that catalyzes the reversible dehydration of 2-phospho-D-glycerate (PGA1) to yield PEP in the glycolytic pathway, is primarily inhibited by F^- in the presence of inorganic phosphate and Mg^{2+}, causing a block in glycolysis (Figure 1 D).

$$Mg^{2+} + F^- + P_i \rightleftharpoons \text{Enolase}.Mg^{2+}.F^-.P_i \qquad \text{(Qin et al., 2006)}$$

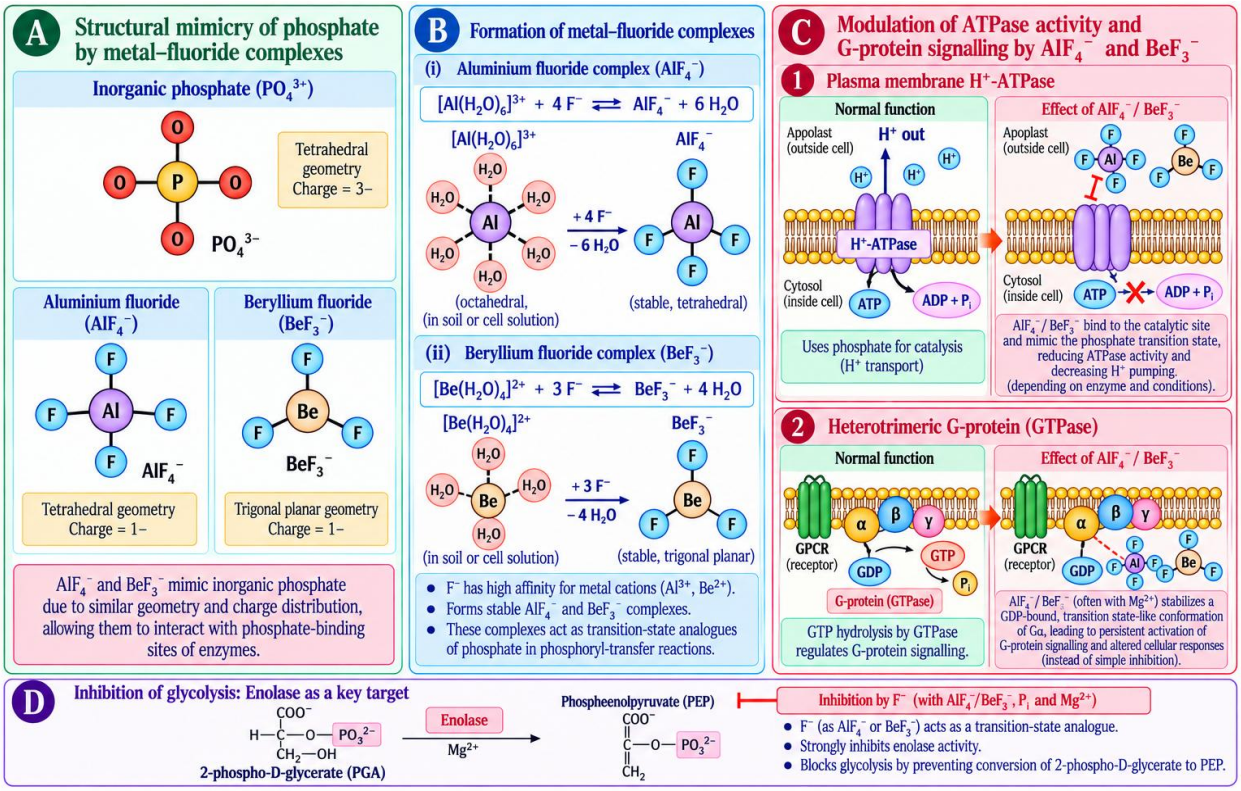


Figure 1. Proposed mechanisms of F^--mediated disruption of phosphate-dependent enzymes and cellular signaling in plants and animals. (A) Structural comparison of inorganic phosphate (PO_4^{3-}) with tetrahedral aluminium fluoride (AlF_4^-) and beryllium fluoride (BeF_3^-) complexes, illustrating their geometric similarity with phosphate. (B) Formation of metal–fluoride complexes through coordination of F^- ions with Al^{3+} and Be^{2+}. (C) AlF_4^- can mimic the γ-phosphate transition state of ATP/GTP hydrolysis, potentially stabilizing catalytic intermediates and altering the activities of plasma membrane H^+-ATPases and heterotrimeric G-proteins, thereby perturbing proton transport and cellular signaling. (D) Fluoride-mediated inhibition of Mg^{2+}-dependent enolase activity, impairing the conversion of 2-phosphoglycerate to phosphoenolpyruvate and consequently disrupting glycolysis.

Phosphatases: Including phosphoserine phosphatase, inhibited by metal-F- complexes. Kinases: Such as phosphoglycerate kinase (PGK) and protein kinases, which transfer phosphate from ATP. ATPases and GTPases: Including myosin and small G proteins, which are inhibited by AlF_4 or

BeF_3 acting as an ADP-phosphate analogue. Phosphorylases and Mutases: Including β-phosphoglucomutase (βPGM), where metal fluorides mimic the phosphoryl transfer transition state. Inorganic Pyrophosphatase (PPase): Strongly inhibited by F^-, particularly in the presence of pyrophosphate (Pellegrini, et al., 2024). These F^- complexes mimic the trigonal bipyramidal transition state of the phosphoryl group in the active site of these enzymes.

Experimental studies show disturbances in amino-acid, fatty-acid, and energy metabolism in bone marrow stem cells and major organs (kidney, liver, brain, heart), as well as alterations in gut microbiota (Wang et al., 2022; Zhao et al., 2022; Zhou et al., 2023). In plants, F^- is non-essential and induces phytotoxicity at molecular, cellular, and physiological levels. Fluoride binds to protein amino-acid side chains, disrupting folding and function, while F^--induced oxidative stress generates reactive oxygen species (ROS) leading to irreversible protein carbonylation (Fig. 2).

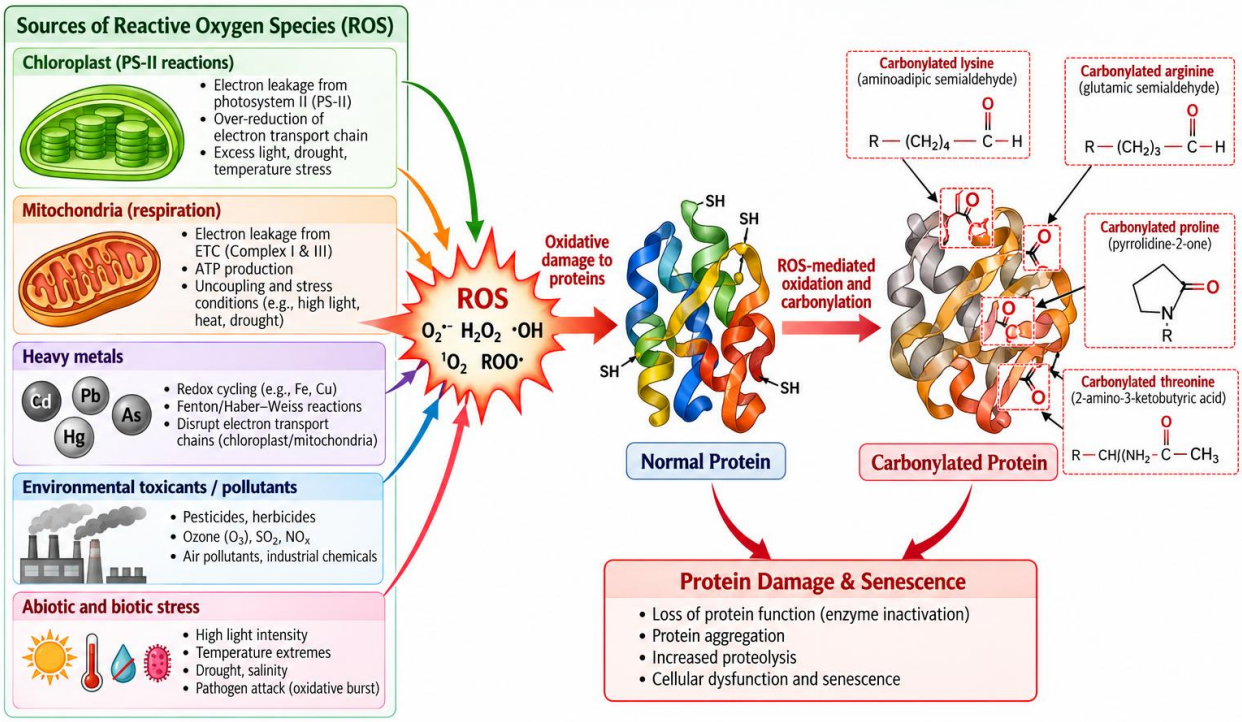


Figure 2. General schematic representation of ROS-mediated protein carbonylation and its physiological consequences in plants. ROS generated in chloroplasts and mitochondria as well as through Fenton type reaction* under heavy metal exposure, environmental pollutants, and abiotic or biotic stresses induces oxidative modifications of cellular proteins. Elevated ROS levels, including superoxide ($O_2\bullet^-$), hydrogen peroxide (H_2O_2), and hydroxyl radicals (•OH), promote irreversible carbonylation of susceptible amino acid residues, particularly lysine, arginine, proline, and threonine. The resulting protein carbonyl derivatives contribute to enzyme inactivation, protein aggregation, enhanced proteolysis, and cellular dysfunction, eventually accelerating plant senescence.

*Fenton type reaction: $Fe^{2+} + H_2O_2 \rightarrow Fe^{3+} + \bullet OH + OH^-$ (1); $Fe^{2+} + OH\bullet \rightarrow Fe^{3+} + OH^-$ (2)

In terrestrial plants, F^- toxicity is evident in levels > 10 mg L^{-1}, leading to leaf injury and impaired growth, however the sensitivity depends on species and environmental factors (Shaji et al. 2024). Plants absorb F^- through their roots via passive diffusive process, F^- entering the apoplast of roots, accumulating it within tissues at amounts that exceed those in the environment. Its

accumulation usually depends on soil F^- levels, plant species, and soil properties (Kumar et al. 2021) with F^- accumulations to the level (mg kg^{-1}) of reported up to 2,277 to 2,346 in mature tea leaves (Singh et al., 2018). Although cell wall Ca^{2+} binds to F^-, forming insoluble CaF_2, and the cell membrane repels the negatively charged F^-, HF is formed at the low apoplastic pH due to protonation of F^-, which being lipophilic, enters the cytoplasm through the plasma membrane easily. F^- easily passes the endodermal barrier, and through symplastic transport, enters the vascular tissues and eventually gets transported over long distances to all plant tissues. Fluoride exposure has been reported to induce oxidative stress through the excessive accumulation of reactive oxygen species (ROS). Although the precise molecular mechanisms underlying F^--induced ROS generation are not yet completely resolved, available evidence suggests that F^- can disturb chloroplast and mitochondrial electron-transport processes, thereby promoting electron leakage and the formation of ROS such as superoxide ($O_2^{\bullet-}$) and hydrogen peroxide (H_2O_2). Fluoride may also impair antioxidant defense systems, including SOD, CAT, APX and glutathione-dependent pathways, further contributing to cellular redox imbalance (Figure 3). Unlike redox-active heavy metals such as Fe and Cu, F^- does not directly generate ROS through a Fenton reaction. However, H_2O_2 generated during F^- stress may subsequently participate in Fenton chemistry in the presence of redox-active transition metals, leading to secondary formation of highly reactive hydroxyl radicals (•OH).

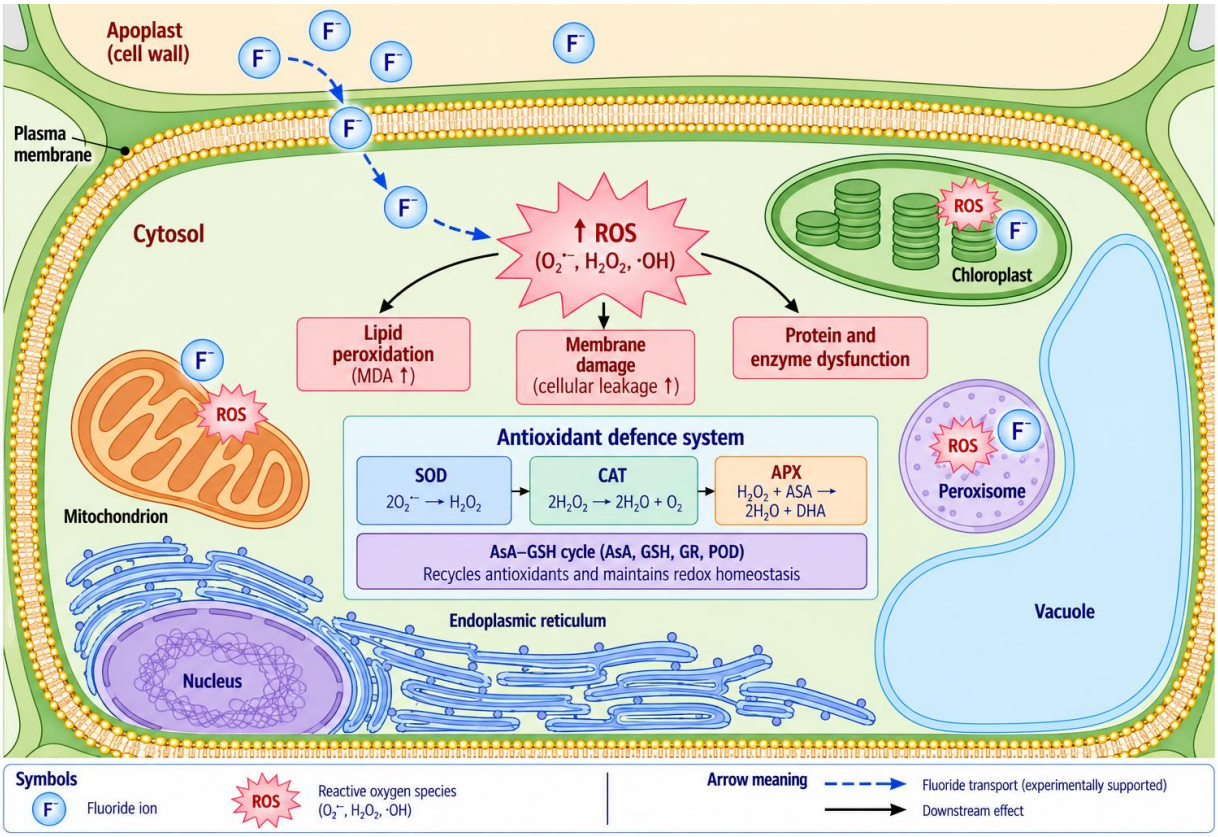


Figure 3. Generalized schematic representation of F^--induced oxidative stress and antioxidant defence mechanism in leaf cells. Fluoride accumulation disrupts cellular redox homeostasis, promoting excessive ROS generation in chloroplasts, mitochondria, and peroxisomes, resulting in lipid peroxidation, membrane damage, and protein dysfunction. Antioxidant enzymes, including superoxide dismutase (SOD), catalase (CAT), and ascorbate peroxidase (APX), together with the ascorbate–glutathione (AsA–GSH) cycle, mitigate oxidative damage by maintaining ROS and redox homeostasis. Dashed blue arrows indicate putative F^- movement, while solid black arrows represent downstream cellular effects.

Further, cellular consequences include reduced cell division and growth and degeneration of organelles—swollen endoplasmic reticulum (ER), mitochondria with decreased matrix density, and tonoplast breakdown (Baunthiyal and Ranghar, 2014; Eleftheriou and Tsekos, 1991; Fornasiero, 2001; Luo et al., 2021; Panda, 2015). One of the common toxic manifestations of F^- in plants is the impairment of both the structure and biochemistry of photosynthetic apparatus (Figure 4). Loss of both chlorophyll a and b accompanied with chlorosis are most common symptoms reported in plants exposed to F^- contamination. The chlorosis usually begins at the leaf margins, and progresses between veins towards the leaf base. Anatomically, the damage first appears in the spongy mesophyll and lower epidermis, followed by chloroplast damage in the palisade parenchyma (Panda, 2015; Verma, et al., 2022; Banerjee, and Roychoudhury, 2019; Junior et al., 2007; Ahmed, et al., 2020; Doley et al, 2004; Singh, and Verma, 2013; Barbier et al, 2010; Rhimi et al., 2016). However, the specific mechanism through which loss of chlorophyll happens, remains to be studied, nevertheless the complexation of Fe by F^- impairs the chlorophyll biosynthesis (Kamiński et al., 2024). The dissociation of Mg from the porphyrin ring of chlorophyll is also caused due to gaseous HF. Fluoride toxicity not only impairs the light absorption by the photosynthetic apparatus but it also affects the photosynthetic electron transport chain. Fluoride ions substitute Cl^- in PSII, which blocks water photolysis and generates ROS thus total quantum efficiency of PSII is reduced due to inhibited Hill reaction (Haddy et al., 2018).

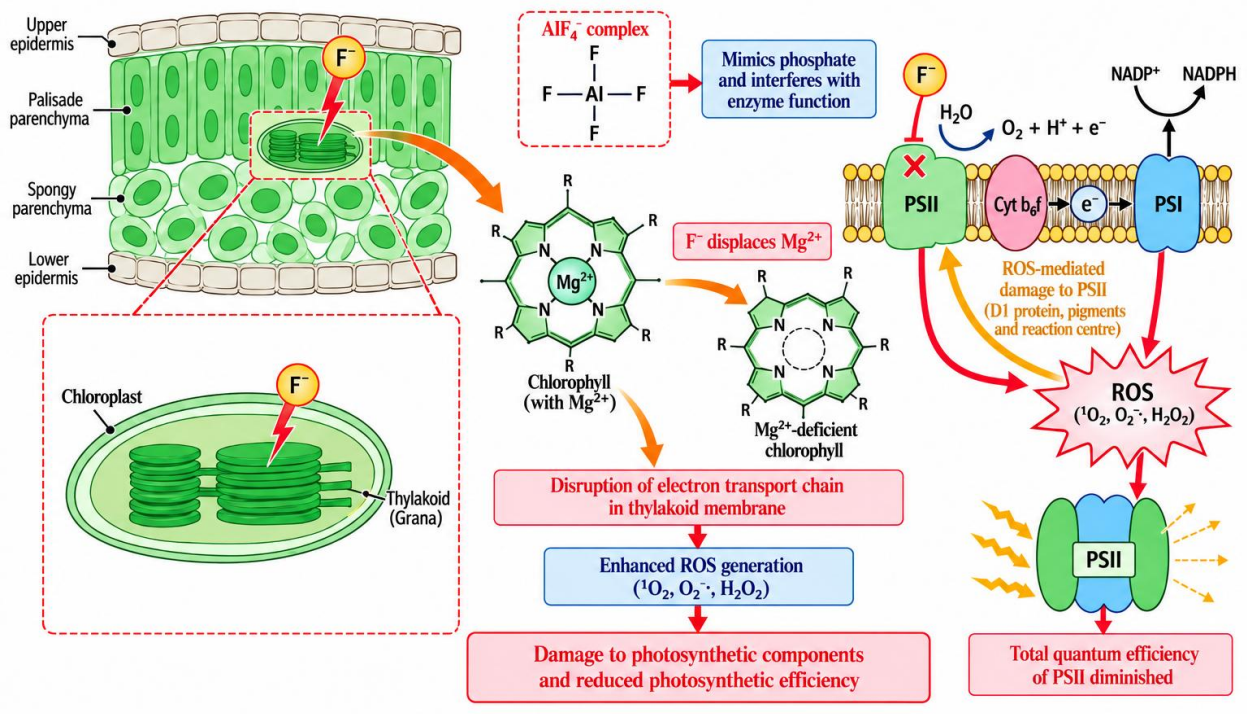


Figure 4. Proposed mechanisms of F^--induced disruption of the photosynthetic apparatus in plants. Fluoride accumulation in leaf mesophyll cells may impair chloroplast structure and function through aluminium–fluoride (AlF_4^-) complex-mediated enzyme inhibition, perturbation of chlorophyll-associated Mg^{2+} homeostasis, and disruption of thylakoid electron transport. Impaired photosystem II (PSII) activity and electron transport promote ROS accumulation, including superoxide ($O_2\bullet^-$), singlet oxygen ($^1O_2$), and hydrogen peroxide (H_2O_2). ROS-mediated oxidative damage to photosynthetic pigments, proteins, and reaction centres further compromises PSII photochemistry, reducing its quantum efficiency and overall photosynthetic performance.

1.3 Interference of F^- with plant nutrients and uptake

The uptake of nutrients and enzyme activities necessary for the assimilation of minerals are disrupted owing to F^- (Gadi et al., 2020; Zouari et al., 2017). F^- toxicity results in decreased photosynthetic activity, enzyme inhibition, and disruptions in the uptake of nutrients and water suggesting that F^- affects the homeostasis of several vital nutrients, probably adversely affecting the absorption of nitrogen, phosphorus, and other minerals (Gadi et al., 2020; Sharma and Kaur, 2018) (Figure 5). Phytotoxic concentrations of F^- also affect plant physiological processes broadly by altering mineral nutrition under stress. For instance, it influences nutrient transport mechanisms, reducing the efficacy of nutrient uptake and assimilation, which can compound the stress effects caused by environmental factors such as drought or soil pollution (Haydon et al., 2015; Rouphael et al., 2012). Nutrient availability and uptake kinetics can be altered when F interacts with other plant nutrients as F^- competes for the uptake sites or interfere with transport mechanisms of other anions such as phosphate and nitrate. Recent studies reveal that F^- induced stress compromises the root membrane integrity, indirectly resulting in the reduced NO_3^- assimilation efficiency (Zhang et al., 2025).

Most plant nutrients are the mineral ions which serve as the components and activators of different biomolecules like chlorophyll and enzyme cofactors, functioning as signalling molecules and this coordinate various metabolic activities (Gadi et al., 2020). F^- is known to retard the water uptake and transport to plants, lowering the relative water content and consequently the stomatal conductance (Elloumi et al., 2017). Few recent research studies have reported that the application of F^- lowers the bivalent cations Ca^{2+} and Mg^{2+} in leaves of *Amygdalus communis* seedlings (Elloumi et al., 2005). Furthermore, F^- accumulation was found to elevate the contents of Na^+, Mn^{2+} and $Fe^{2+/3+}$while simultaneously reducing the levels of K^+, Ca^{2+}, and Mg^{2+} in *Salicornia brachiata*, a halophyte grown under hydroponic cultures (Reddy and Kaur 2008). Complexation reaction of F^- with bivalent cations of Ca^{+2}, Mg^{2+} and Mn^{+2} is the primary mechanism to produce deficiency of the ions, which are required as cofactors for activation of many enzymes of metabolic reactions and signalling pathways in plants (Steven et al., 1997; Banerjee and Roychoudhury 2019b).

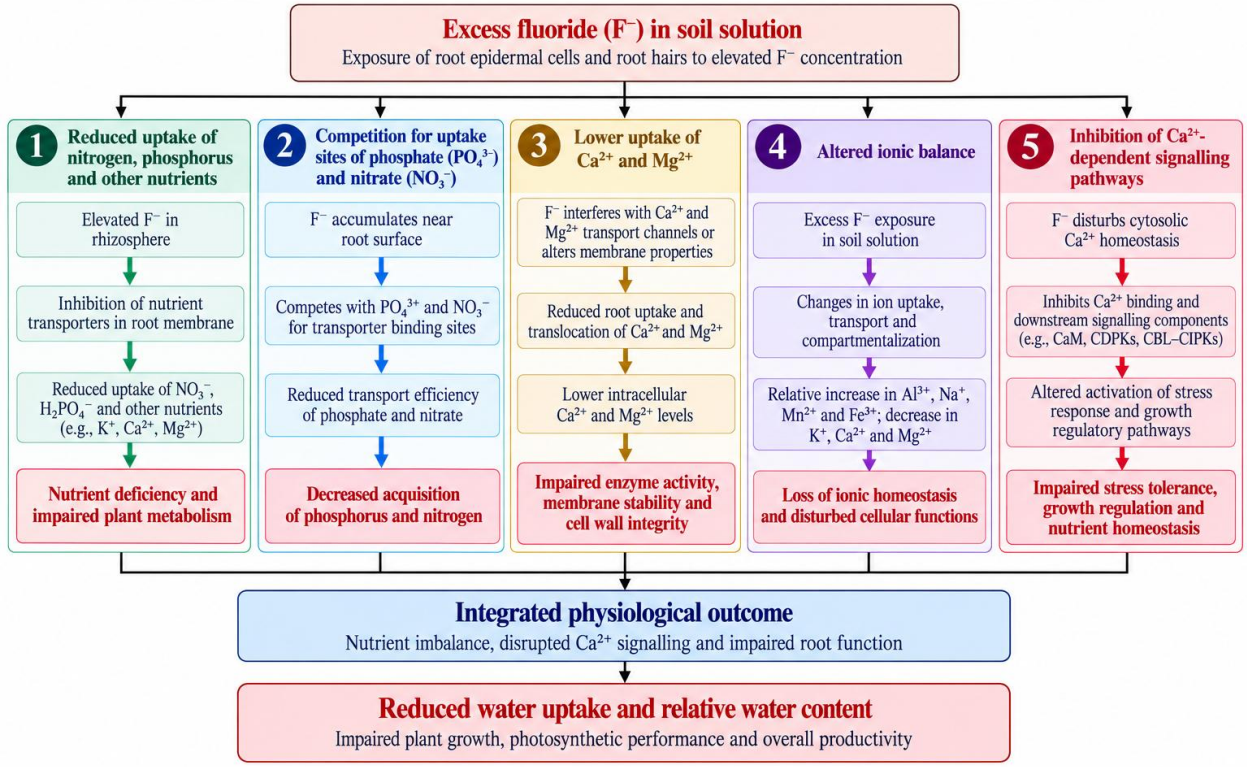


Figure 5. Proposed generalized effects of F^- stress on nutrient homeostasis, Ca^{2+} signaling, and water uptake in plants. Excess F^- in the rhizosphere may impair acquisition of several vital nutrients by altering the root membrane transport, eventually disrupting the cellular PO_4^- and NO_3^- uptake, and Ca^{2+} and Mg^{2+} homeostasis. Fluoride-induced ionic imbalance and perturbation of Ca^{2+}-dependent signaling pathways can further disrupt metabolic regulation and root function. Collectively, these alterations may compromise plant water uptake, relative water content, photosynthetic performance, and overall growth.

Moreover, F^- shows synergistic effects when present with other minerals since it is evident that F^- along with Cadmium (Cd) results in reduced growth and Cu^{2+} uptake while enhanced Zn^{+2} uptake (Chen et al. 2017). The binding of F^- with signalling molecules Ca^{+2} within plant cells

inhibits the Ca^{2+} dependent signalling pathways, thereby alteration of Ca^{2+} mediated signalling inactivates transcription factors and gene expression consequently disturbs metabolic pathways. (Banerjee and Roychowdhury 2019b).

2.0 Fluoride transporters: Putative Vs Bona-fide

Molecular studies have increasingly revealed that F^- transport in plants involves both dedicated F^--export systems and broader-spectrum anion transport proteins (Table 1). Among the identified proteins, the FLUORIDE EXPORTER (FEX) represents the best-characterized and most compelling plant F^--specific transport system. FEX homologues are widely distributed among plants and have been demonstrated to mediate F^- efflux and enhance F^- tolerance. Genetic and physiological studies, together with radioisotopic ($^{18}F^-$) imaging, have provided evidence for the role of FEX in regulating F^- movement and accumulation, while recent structural and electrophysiological investigations have established FEX as a highly selective F^- channel.

Table 1: Fluoride transporter inventory

Transporter	Species / systems	Localization	Transport / direction	Fluoride-related evidence	Class	Primary citation
FEX	Arabidopsis; yeast	Plasma membrane (tested systems)	F^- efflux; native kinetics may vary	Functional complementation and F- -sensitive mutants	A	Tausta et al. (2021)
CsFEX; CsFEX1/2	Tea; heterologous systems	Plasma-membrane-associated; verify each construct	F^- export supported; native tissue flux incompletely resolved	Fluoride response and heterologous resistance/function	A/B	Zhu et al. (2019); Song et al. (2020)
CsABCB9 (TEA013868.1)	Tea; E. coli, Xenopus, Arabidopsis	Chloroplast-associated	Proposed chloroplast ↔ cytosol F^- redistribution; direction unverified	Heterologous accumulation; localization; transgenic tolerance	B	Luo et al. (2022)
CsALMT6	Tea; heterologous assays and silencing	Plasma membrane (reported)	Direct F^- permeability/direction unproven	Fluoride tolerance and altered accumulation after silencing	B	Li et al. (2025), Horticulture Research
CsALMT14	Tea; yeast, Arabidopsis, silencing	Plasma membrane (reported)	Direct F^- permeability/direction unproven	Reduced accumulation in heterologous assays; malate/citrate effects	B	Li et al. (2025), Ecotoxicol. Environ. Saf.
CLCF	Bacteria	Bacterial cytoplasmic membrane	F^-/H^+ antiport; direct microbial F- export	Transport and structural/biophysical assays	A (microbial)	Stockbridge et al. (2012); Last et al. (2018)
AtCLCa–f	Arabidopsis	Isoform-dependent: tonoplast and other internal membranes	Cl^-/NO_3^- and organellar ion functions; no established F^- flux	No F- -specific transport shown in supplied evidence	C	Plant CLC literature; F^- primary study not established
NRT1	Various plants	Isoform-dependent; often plasma membrane	Nitrate uptake/vascular redistribution; F^- unverified	No direct F^- substrate evidence	C	Nitrate transport literature
NPF (NRT1/PTR); CsNPF2.3	Various plants; CsNPF2.3 in tea	CsNPF2.3: plasma membrane	CsNPF2.3 linked to F^- influx; H^+ coupling unverified	Yeast F- accumulation and tea-root genetic evidence	B (CsNPF2.3)	Niu et al. (2025)
NRT2	Various plants	Plasma membrane for characterized uptake isoforms	High-affinity nitrate uptake; F^- unverified	No F- -specific substrate evidence	C	NRT2 nitrate literature

Classes: A = F- transport supported by functional assays in a defined system; B = F- -related functional phenotype, but native membrane flux or direction unresolved; C = candidate/indirect relevance without demonstrated F- transport. A/B indicates differences among individual family members or experimental systems.

In addition to FEX, members of several established anion-transporter families, including chloride channels (CLC), aluminum-activated malate transporters (ALMT), ATP-binding cassette (ABC) transporters and nitrate transporter/peptide transporter (NRT/NPF) proteins, have been implicated in F^- transport or homeostasis. Their possible involvement is biologically plausible because these proteins mediate the transport of inorganic or organic anions and can influence membrane ion gradients, intracellular compartmentalization and anion distribution. However, the strength of evidence differs considerably among these transporter families. Whereas FEX has direct experimental support for F^- transport, the involvement of CLC, ALMT, NRT/NPF and ABC proteins in plant F^- transport remains comparatively less well established and, in many cases, is inferred from their substrate specificity, expression patterns, mutant phenotypes or indirect physiological responses. Importantly, transcriptional induction of an anion transporter under F- stress alone cannot establish its ability to transport F^- directly.

2.1 FEX transporters

Fluoride Exporter (FEX) are the transmembrane transport proteins that confer F^- tolerance by facilitating the efflux of toxic F^- ions from the cytoplasm to the extracellular environment (Berbasova et al., 2017; Tausta et al., 2021). F^- is a ubiquitous environmental xenobiotic that inhibits enzymes relying on hydroxyl-forming intermediates or reactive phosphate, which are involved in vital biochemical metabolism i.e., glycolysis, phosphorylation, and nucleotide synthesis because of its ability of non-nucleophilic hydroxide mimicking, because of its small atomic radius and high basicity. Also, its ability of forming AlF_4^- complex with Al^{+3} in an acidic environment which act as an analog of phosphate ion (PO_4^-) that can serve as a transition state mimic to inhibit phosphoryl transfer reaction (Berbasova et al., 2017). **(Table 1.)**

FEX are transmembrane efflux proteins which function as an ion transporters prevalently in bacteria and yeast in order to expel the F^- (Tausta et al., 2021). FEX homologs are ubiquitously present across all domains of life. In prokaryotes, these F^- channels are termed as Fluc (formerly *crcB*), whereas eukaryotes utilize the F^- exporters FEX (Berbasova et al., 2017). FEX proteins function as highly selective ion channels, exhibiting at least 10-fold selectivity for F^- over Cl^-, and with its bacterial homologs (Fluc) exhibiting >10,000-fold selectivity (Berbasova et al., 2017; Tausta et al., 2021). In yeast, FEX deletion results in ~1000-fold increased F^- sensitivity, with IC_{50} values dropping from 70 mM in wild-type to 60 µM in knockouts (Tausta et al., 2021). Thus, the FEX channels are essential in prokaryotes for surviving in F^- rich toxic environments.

In plants, FEX homologs have been identified in every investigated plant genome thus far (Tausta et al., 2021). Genome-wide investigations have revealed 31 FEX genes across 19 species, encompassing model plants (*Arabidopsis thaliana, Oryza sativa*), various crops (*Glycine max, Phaseolus vulgaris, Vitis vinifera, Solanum tuberosum, Lactuca sativa*), and basal land plants such as *Physcomitrium patens* (Tausta et al., 2021; Agarwal et al., 2021). While most plant genomes consists 1-2 FEX genes, *Triticum aestivum* and *Vigna unguiculata* contain 3-4 copies, potentially

arising due to the gene duplication events probably occurred during 8500 to 9000 years ago in holocene epoch when wheat was supposed to undergo hexaploidization and around 50 to 60 million years ago in the Paleogene Period, followed by a papilionoid duplication event in *Vigna unguiculata* (Agarwal et al., 2021; Levy and Feldman, 2006; Cronk et al., 2006). In fungi, *Saccharomyces cerevisiae* possesses two genes (*FEX1* and *FEX2*) with high sequence similarity, and functional homologs are also reported in *Neurospora crassa* and *Candida albicans* (Berbasova et al., 2017).
Among animals, FEX-like genes are present in aquatic organisms like the sea sponge *Amphimedon queenslandica*, though they may be absent in terrestrial animals or governed by alternative tolerance mechanisms (Berbasova et al., 2017).
In the F- hyperaccumulator *Camellia sinensis* (tea plant), multiple FEX members including *Cs*FEX, *Cs*FEX1, and CsFEX2 have been characterized; notably, CsFEX2 exhibits F^- -inducibility and is primarily associated with low-F^- cultivars (Song et al., 2020; Zhu et al., 2019).

2.1.1 Structural details of FEX homologs:

Bacterial Fluc is a double-barreled channel formed as a result of antiparallel dimerization of two identical or similar subunits containing the two functional pores (Figure 6A). Each monomer consist of four transmembrane (TM) α-helices (Berbasova et al., 2017). The 3D crystal structure using the monobodies (Ec2-S9 from *E.coli*; Bpe-Lc2 and Bpe-S7 from *B. pertussis*) as crystallization chaperons of bacterial exporter fluc channels in *E.coli* and *B. pertussis* revealed a double-barreled two-pore assembly of F^- specific ion channels (Stockbridge et al., 2013; Stockbridge et al., 2015 ; Berbasova et al., 2017). These crystal structures also exhibited that transmembrane helix 3 (TM3), a highly conserved helix (TGxxxGLTTFSTFxxxE) is divided into two halves, TM3a and TM3b by a 6-residue non-helical segment located roughly at the membrane's center. The two TM3 half helices from distinct monomers physically separate the two pores, with residues on two sides of the same helix occupying positions in each pore. This arrangement is achieved by the formation of an antiparallel dimer because two TM3b helices are essential for the dual pore architecture. Two TM3 helices from separate monomers cross at the center of the membrane and form a putative sodium binding site, which signifies that the cation is structurally important (Stockbridge et al., 2015; Berbasova et al., 2017). The pores of bacterial Fluc channels are proposed to utilize aromatic and hydrogen bond donating amino acids. For instance, highly conserved phenylalanines located within the TM3 facing into the pore and adopting the side-to-face 'box'-like arrangement for interaction with F^-. While the residues within the TM4 facing the pore are mostly different H-bond donors of low sequence identity (Figure 6 B). Every 4^{th} residue in TM4 varies between Asparagine (N), Serine (S), Threonine (T), Histidine (H) or Tyrosine (Y), which is suggested to provide a polar track required for identification of F^- ions (Stockbridge et al., 2015; Berbasova et al., 2017; Last et al., 2016). The crystal structure also revealed there is Na^+ binding site, coordinated by four backbone carbonyl groups from Ser/Thr residues for stabilization of dimer interface (Berbasova et al., 2017; McIlwain et al., 2021).

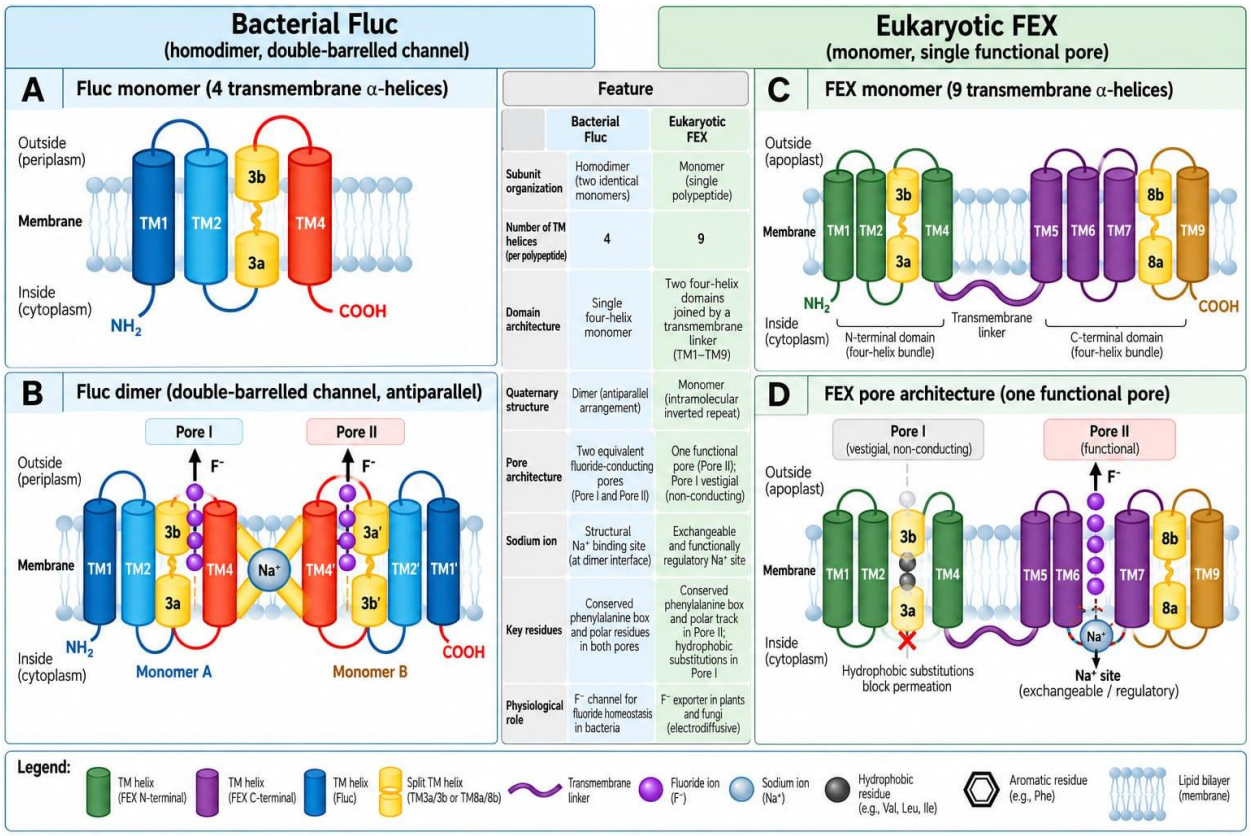


Figure 6. Comparative structural organization and F^- transport architecture of bacterial Fluc channels and eukaryotic FEX exporters. (A) Bacterial Fluc monomer comprising four transmembrane (TM) α-helices, with TM3 divided into TM3a and TM3b by a short non-helical segment. (B) Antiparallel dimerization of two Fluc monomers forms a double-barreled channel containing two functional F- -conducting pores and a structural Na^+-binding site at the dimer interface. (C) Eukaryotic FEX consists of a single polypeptide with nine TM helices, organized into two homologous four-helix domains connected by a transmembrane linker. (D) Unlike bacterial Fluc, FEX retains one functional F- -exporting pore (Pore II), whereas Pore I is non-conducting due to substitutions in key pore-lining residues. Conserved aromatic and polar residues contribute to F^- selectivity and permeation. The schematic highlights the structural and functional divergence of Fluc and FEX proteins during evolution (Stockbridge et al., 2015; Last et al., 2016; Berbasova et al., 2017; Banerjee and Roychoudhury, 2019; Tausta et al., 2021; Kang et al., 2025).

In contrast, eukaryotic FEX is a monomer resulting from covalent fusion and gene duplication of two homologous domains (each resembling a Fluc monomer) joined by a transmembrane linker that forces an antiparallel orientation as an inverted repeat (Berbasova et al., 2017; Tausta et al., 2021) (Figure 6 C). The single polypeptide chain contains nine transmembrane helices with the N-terminal and C-terminal four-helix domains forced into antiparallel orientation by a transmembrane linker helix (Banerjee and Roychoudhury, 2019; Agarwal et al., 2021; Kang et al., 2025). While FEX shares the exact core fold of Fluc but key architectural differences emerged, specifically only one pore (Pore II) remains functional for F^- transport, whereas the symmetrical pore I has degenerated into a non-conducting vestigial remnant (Berbasova et al., 2017) (Figure 6D). Actually, the functional pore retains essential coordinating residues including the phenylalanine box and polar track whereas the vestigial pore has accumulated hydrophobic substitutions that obstruct the pathway (Tausta et al., 2021). The non-functionality of Pore I has been the result of evolutionary shift due to the mutations in amino acid residues which forces the

pore to adopt hydrophobicity to account for the existing functional redundancy and selection pressure. Furthermore, the Na^+-binding niche, structural in Fluc, becomes exchangeable and functionally regulatory in FEX (Kang et al., 2025).

2.1.2 Fluoride permeation mechanism through FEX exporters

The permeation pathway initiates at the electronegative extracellular vestibule, where F^- ions encounter a conserved arginine residue (R23 in bacterial homologs) that electrostatically guides anions toward the pore entry (Stockbridge et al., 2015; Kang et al., 2025). From the vestibule, F^- moves into a narrow, dehydrated crevice lined by a "polar track" of hydrogen bond-donating residues—S, T, N, and H—spaced every four residues along transmembrane helices (McIlwain et al., 2021; Stockbridge et al., 2015). Crucially, the permeation pathway features a conserved "phenylalanine box," where two aromatic residues (F96 and F330 in yeast FEX) present their electropositive quadrupolar ring edges to coordinate F^- ions via anion-π interactions, compensating for the high energetic cost of F^- dehydration (Berbasova et al., 2017; Last et al., 2016). Structural and computational studies suggest a "water-mediated knock-on" mechanism, wherein alternating F^- ions and water molecules occupy adjacent binding sites (designated F_1 and F_2), and electrostatic repulsion between ions facilitates rapid throughput (Zhang et al., 2023; Kang et al., 2025). Transport is driven passively by the negative-inside membrane potential, which favors anion efflux, and in plant FEX, activity is further coupled to proton gradients, with acidic extracellular pH enhancing export (Song et al., 2020). Single-channel recordings reveal F^- flux rates of ~10^5–10^6 ions per second, confirming channel-mediated conduction (Stockbridge et al., 2013; Tausta et al., 2021). Remarkably, FEX achieves >10,000-fold selectivity for F- over Cl^- through a combination of pore constriction, precise coordination geometry requiring fewer ligands, and the unique polarizability of aromatic side chains (McIlwain et al., 2021; Kang et al., 2025). Thus, FEX proteins provide an specific molecular solution for F^- extrusion, enabling eukaryotic cells to maintain cytoplasmic F^- at non-toxic levels despite environmental exposure.

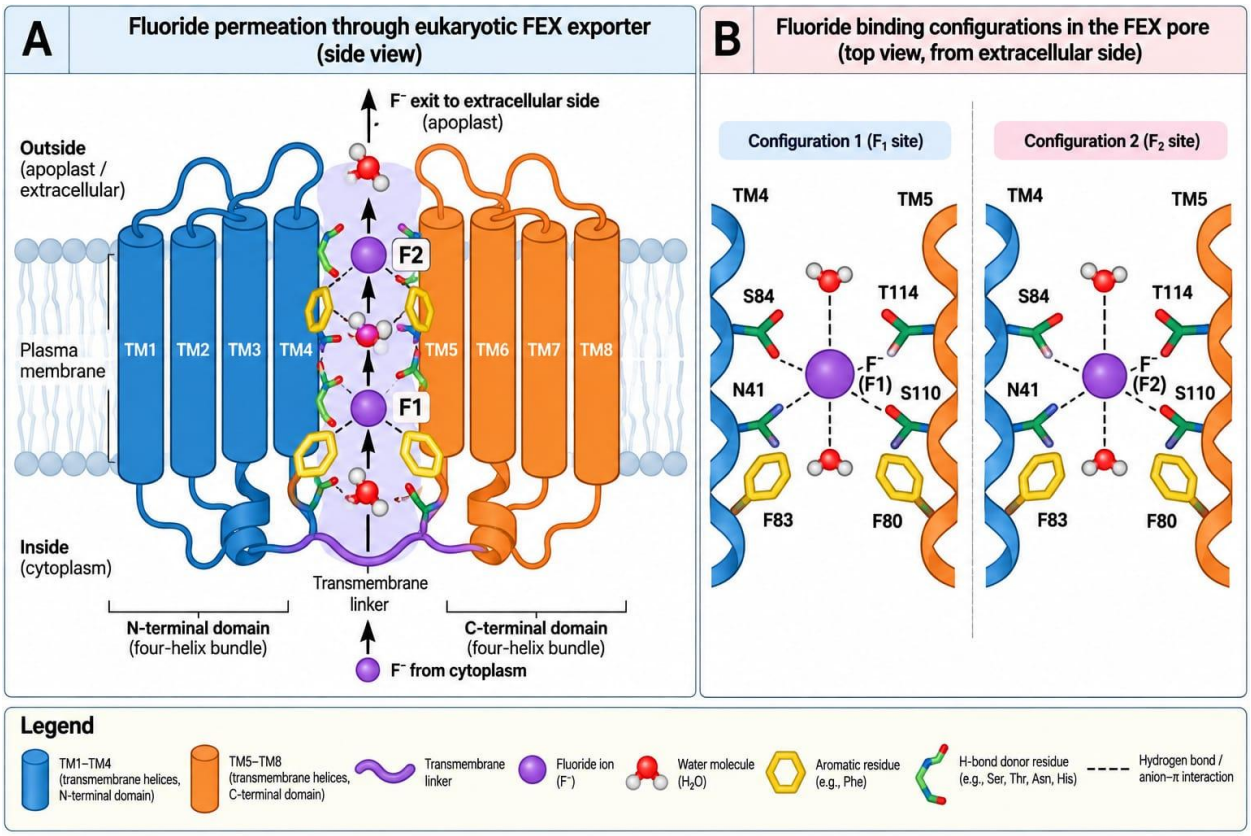


Figure 7. Structural organization and proposed F^- permeation mechanism of eukaryotic FEX exporters. (A) Schematic representation of the FEX exporter comprising N- and C-terminal four-helix domains connected by a transmembrane linker, forming a F^--selective permeation pathway. Fluoride efflux from the cytoplasm to the extracellular environment is facilitated by conserved aromatic residues and polar hydrogen-bond donors. (B) Proposed F^--binding configurations at the F_1 and F_2 sites, illustrating interactions with conserved phenylalanine residues, polar amino acids, and water molecules that may contribute to F^- coordination and permeation. The proposed transport mechanism involves sequential ion occupancy and water-mediated interactions, although the precise molecular dynamics remain under investigation (Stockbridge et al., 2015; Last et al., 2016; Berbasova et al., 2017; McIlwain et al., 2021; Zhang et al., 2023; Kang et al., 2025).

Table 2. Fluoride-mediated inhibition of phosphotransferase enzymes through formation of transition-state analogue metal–F- complexes.

	Target Enzyme / System	Organism / Source	Metal–Fluoride Complex	Representative Inhibition Mechanism / Equation	Reference
1	PEP-dependent phosphotransferase system (PTS; indirect)	*Streptococcus sanguis*	Indirect via enolase inhibition	$F^- \rightarrow$ Enolase inhibition $\rightarrow$ PEP $\downarrow \rightarrow$ PTS activity $\downarrow \rightarrow$ Sugar uptake $\downarrow$	Hata et al. (1990)
2	F_1-ATPase	Bovine heart mitochondria	AlF_4^- / BeF_3^-	E-ATP + $AlF_4^- \rightarrow$ E-ADP–AlF_4^- (stable inactive complex)	Dupuis et al. (1989)

3	Acetate kinase	*Methanosarcina thermophila*	AlF_4^-	E + MgADP + acetate + AlF_4^- → E·MgADP·AlF_4^-·acetate (abortive complex)	Miles et al. (2002)
4	General phosphotransferases and GTPases	Various organisms	AlF_4^-, BeF_3^-, MgF_3^-	E + NDP + MF_x → E–NDP–MF_x (universal transition-state mimic)	Li (2003)
5	Enolase	*Saccharomyces cerevisiae*	$Mg_2F_2P_i$ (EFPIC)	Enolase + $2F^-$ + P_i + $2Mg^{2+}$ → Enolase–$Mg_2F_2P_i$ (inactive EFPIC complex)	Qin et al. (2006)
6	Phosphoenolpyruvate synthetase (PEPs)	Recombinant bacterial enzyme	MgF_3^-	PEPs + MgF_3^- + ATP → PEPs·MgF_3^-·ATP (abortive transition-state analogue)	McCormick & Jakeman (2015)

Legend: *E, enzyme; NDP, nucleoside diphosphate; MF_x, generic metal–F- transition-state analogue; PEP, phosphoenolpyruvate; PTS, phosphotransferase system; P_i, inorganic*

2.1.3 Recent studies in FEX exporter protein:

Over the past several years, scientific advances have fundamentally reshaped our understanding of FEX proteins mostly in eukaryotes. The cryo-electron microscopy structure of *Candida albicans* FEX, solved at 4.0 Å resolution, revealed that eukaryotic FEX adopts an inverted repeat architecture with a single functional pore, as the symmetry-related second pore has degenerated into a non-conducting vestigial remnant lined by hydrophobic residues (Kang et al., 2025). This structural analysis further uncovered that FEX possesses an electronegative extracellular vestibule—strikingly different from the electropositive vestibules of bacterial Flucs—and a conserved Na-binding "niche" motif that is solvent-accessible and exchangeable, with Na binding exhibiting a dissociation constant of ~0.4 mM and being required for full F^- efflux activity (Kang et al., 2025). Complementary solid-state NMR studies on Fluc-Ec1 in native-like liposomes provided the first direct experimental evidence that F^- occupies the F_2 sites while water molecules reside at the F_1 positions, challenging earlier crystallographic assignments and supporting a "water-mediated knock-on" permeation mechanism wherein alternating F^- ions and water molecules traverse the pore (Zhang et al., 2023). The study also identified loop 1 as a critical dynamic hotspot for channel gating, with mutational disruption of loop 1 residues (N27A, I33S/L35S) abrogating F^- transport (Zhang et al., 2023).

In planta, positron emission tomography (PET) imaging of [^{18}F] fluoride movement in *Arabidopsis* revealed that FEX functions not by root exclusion or vacuolar sequestration, but by facilitating F^- efflux from individual cells along the transpiration stream, enabling bulk flow to apical tissues where F^- may be released via hydathodes or stomata (Tausta et al., 2024). Furthermore, transcriptional regulation of FEX has been shown to involve the CAM1-CAMTA module, wherein Ca^{2+}-activated calmodulin interacts with CAMTA transcription factors that bind the G-box (CACGTC) cis-element in the FEX1 promoter, functioning as a transcriptional repressor under non-stress conditions (Li et al., 2025) (Figure 8). Collectively, these advances—from high-resolution structures and dynamic NMR spectroscopy to live-imaging and regulatory network dissection—have transformed FEX from a mere F^- efflux conduit, to a paradigm for understanding ion channel evolution, substrate selectivity, and multi-level regulation in plant stress physiology.

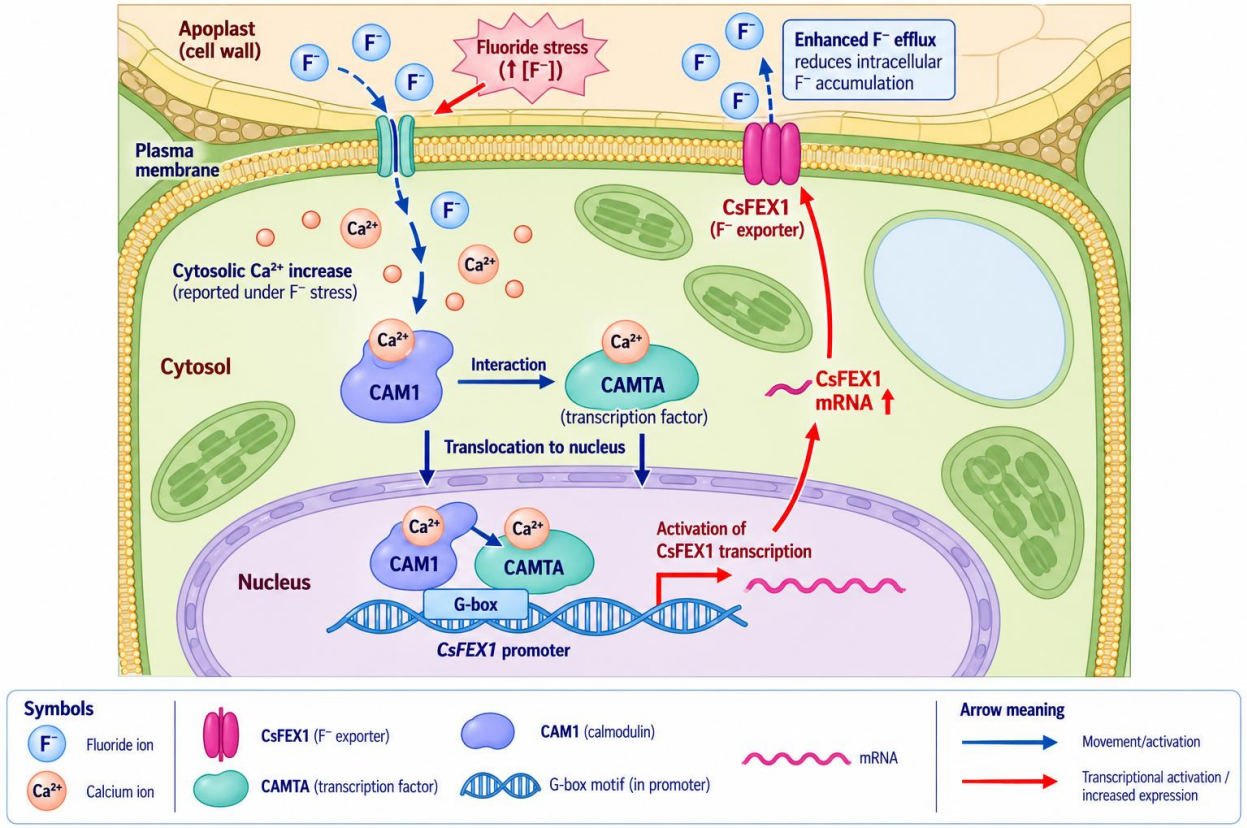


Figure 8. Proposed Ca^{2+}-dependent CAM1–CAMTA–CsFEX1 regulatory module mediating F^- tolerance in tea (*Camellia sinensis*) leaf cells. Fluoride stress elevates cytosolic Ca^{2+} levels, facilitating Ca^{2+}-dependent CAM1–CAMTA interaction and subsequent activation of CsFEX1 transcription through CAMTA binding to the G-box cis-regulatory element in its promoter. Enhanced CsFEX1 expression promotes $F^=$ efflux across the plasma membrane, limiting the intracellular F^- accumulation and contributes towards F^- tolerance. Blue arrows indicate molecular movement and signaling events, whereas red arrows denote transcriptional activation and F^- export.

2.2 CLC transporters

The CLC superfamily consists broadly-distributed anion transport proteins that function either as chloride channels or as proton-coupled anion antiporters, playing multiple physiological roles across all kingdoms of life (Jentsch and Pusch, 2018; McIlwain et al., 2021). In prokaryotes such as bacteria, CLCs show resilience to extreme acidic niches, while in mammals, they facilitate skeletal muscle membrane potential maintenance, endosomal and lysosomal acidification, and renal solute concentration (Accardi and Miller, 2004; McIlwain et al., 2021). Structurally, CLC proteins assemble as homodimers, with each subunit containing 16–18 transmembrane α-helices organised as two internally duplicated seven-helix domains oriented in opposite topology (Dutzler et al., 2002; Last et al., 2018). The transport mechanism of Cl^-/H^+ antiporters involves a conserved "gating glutamate" (E148 in CLC-ec1) that undergoes protonation-dependent rotameric transitions, alternatively opening the pathway to extracellular or intracellular solutions (Accardi et al., 2005; Dutzler et al., 2003). An additional intracellular glutamate (E203) participates in proton relay from the cytoplasmic side via transient water wires (Lim and Miller, 2013). Anions bind at three distinct sites (S_{ext}, S_{cen}, S_{int}) coordinated by backbone amides and side-chain hydroxyls of

conserved serine and tyrosine residues, with a 2:1 Cl^-/H^+ exchange stoichiometry (Picollo et al., 2009; Accardi and Miller, 2004). The recently discovered CLC^F clade dissects from this canonical mechanism, exhibiting 1:1 F^-/H^+ stoichiometry and unique fluoride-selective coordination chemistry (Stockbridge et al., 2012; Last et al., 2018).

2.2.1 CLC^F Antiporters: Biological Distribution, Physiological Role, and Phylogenetic Types

These CLC^F proteins are a phylogenetically distinct bacterial clade within the CLC superfamily, serving the unique role of F^- export via proton-coupled antiport (Stockbridge et al., 2012; Last et al., 2018). These transporters are broadly distributed among both Gram-negative and Gram-positive bacteria, including species such as *Enterococcus casseliflavus*, *Pseudomonas syringae*, *Lactococcus lactis*, and *Pirellula staleyi* (Brammer et al., 2014). Their expression is regulated by F^--responsive riboswitches—conserved RNA elements that bind F^- and upregulate transcription of downstream exporter genes upon cytoplasmic F^- accumulation (Baker et al., 2012; McIlwain et al., 2021). It is the proton motive force (PMF) that act as driving force by which CLC^F antiporters export wherein, one F^- is exchanged for one H^+. Consequently, alleviating the weak acid accumulation effect or ion trapping in cytoplasm of microbes residing in the acidic niches, wherein extracellular HF (pKa=3.4) a weak conjugate acid diffuses across the membrane and dissociates in the neutral cytoplasm (Ji et al., 2014; McIlwain et al., 2021). Phylogenetic analysis resulted in the discovery of two major subclades within the CLC^F family, determined by conserved sequence differences in the anion-coordination region: the "N-T" subclade that is characterized by an asparagine in helix D and a threonine in helix F and the "M-V" subclade on other hand adopt a methionine and valine at equivalent positions (Brammer et al., 2014). The M-V subclade exhibits approximately two-fold higher F^-/Cl^- transport selectivity and tighter F^- binding affinity compared to N-T representatives, making these two residues largely account for the subclade differences as demonstrated by chimeric swap experiments (Brammer et al., 2014).

2.2.2 Thermodynamic and Molecular Basis of F- Selectivity in CLC^F Antiporters

The mechanistically unique achievement of F^- selectivity over Cl^- employs the following thermodynamic and molecular strategies in CLC^F antiporters, making them a unique evolutionary adaptation in prokaryotic world to survive the challenging F^- niche:

I. A dehydrated and under-coordinated binding pocket that favors the smaller fluoride ion.
II. Hydrogen-bond donation from strategically positioned side chains (Y396, E318, T320).
III. The polarizing influence of methionine's sulfur atom.
IV. Active electrostatic participation of the deprotonated gating glutamate in ejecting the bound F^-, thereby coupling selectivity to the transport cycle itself (Last et al., 2018; Chon and Lin, 2024; Mills and Torabifard, 2023).

The transport of F^- over Cl- by CLC^F antiporters poses a thermodynamic paradox due to F^-'s higher dehydration penalty (~111 kcal/mol) over Cl^- (~81 kcal/mol). However, specialized coordination chemistry at the anion-binding sites resolves this issue, with methionine (M79) and tyrosine (Y396) facilitating F^-'s selective translocation. Phylogenetic studies reveal significant differences in residue distribution among CLC^F subclades, impacting transport selectivity. Notably, glutamate E318, absent in Cl^--transport CLCs, enhances F^- selectivity through a protonated hydrogen bond.

The gating glutamate E118 actively influences selectivity by competing with F-, allowing electrostatic expulsion, which is critical for effective transport. Neutralizing E118 mutations reveal the complex balance between binding affinity and the electrostatic push necessary for F^- transport, highlighting that selectivity is not merely about tighter binding but also about the dynamic role of residues in the transport mechanism.

2.2.3 Structural composition

CLC^Fs are known to assemble as homodimers in the membrane with each monomer containing a complete and independently functional transport pathway (McIlwain et al., 2021; Last et al., 2018). The dimer interface is constituted by four transmembrane helices (H, I, P, Q) that are arranged tightly against one another (Figure 9). Studies has revealed that individual tryptophan substitutions at this interface, specifically L376W, create completely monomeric versions that still function at full capacity. This demonstrates that the dimeric structure is not essential for performance and that each monomer can function independently (Last et al., 2018).

Each monomer comprises 14 transmembrane α-helices arranged as two structurally homologous seven-helix domains related by internal inverted symmetry (McIlwain et al., 2021). Two helices (αA and αR) which are seen to present in Cl^--transporting CLCs are absent in CLC^F and several other helices are found shorter than their Cl^--CLC counterparts (Last et al., 2018). The helices are generally tilted relative to the membrane plane, defining electropositive intracellular and extracellular aqueous vestibules of approximately 6–8 Å deep that converge at a central, largely anhydrous ion-coupling region (McIlwain et al., 2021; Last et al., 2018). The Crystal structures of the *Enterococcus casseliflavus* CLC^F homologue have captured the transporter in two distinct conformational states: an inward-open-to-F^-/outward-open-to-H^+ conformation (wild-type) and an inward-open-to-H^+/outward-occluded-to-F^- conformation (V319G mutant) (Last et al., 2018). In the wild-type structure, the gating glutamate E118 attains the Up rotamer position that blocks extracellular access to F^- while exposing the anion-binding sites to the intracellular solution; conversely, in the V319G structure, E118 is in the Down position, occluding F^- from the intracellular side while permitting proton exchange with the cytoplasm (Last et al., 2018). This conformational switching forms the basis of the "windmill" antiport mechanism (Last et al., 2018).

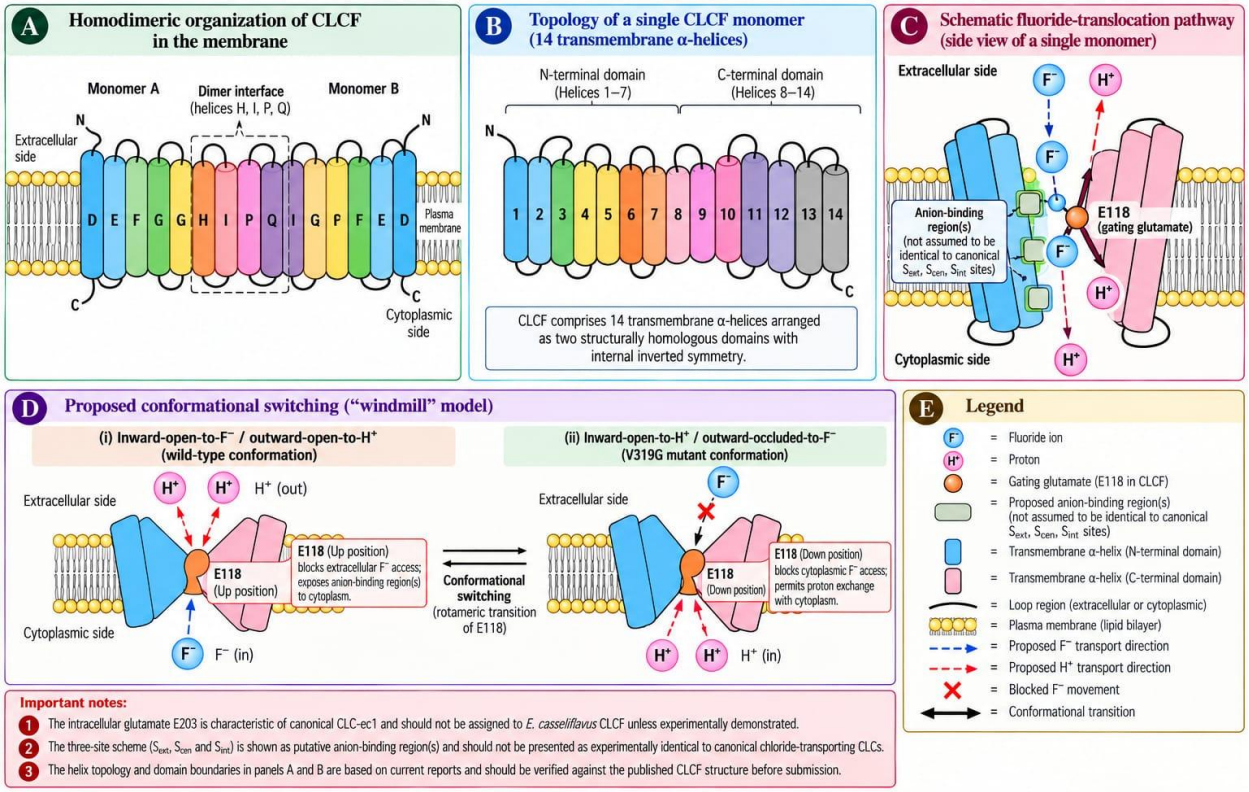


Figure 9. Structural organization and F^-/H^- antiport mechanism of bacterial CLCF transporters. (A) Homodimeric organization of CLCF within the bacterial cytoplasmic membrane, with each monomer containing an independent ion-transport pathway. (B) Structural topology of a CLCF monomer comprising 14 transmembrane α-helices arranged into two inverted-repeat domains. (C) Schematic representation of the F- -translocation pathway, highlighting anion-binding regions and the conserved gating glutamate (E118). (D) Proposed windmill mechanism illustrating conformational switching of E118 between the Up and Down orientations, based on wild-type and V319G mutant structures, respectively. These transitions facilitate alternating F^- accessibility and H^+ exchange, consistent with a 1:1 F^-/H^+ antiport mechanism. The mechanism is derived from bacterial CLCF studies and has not been experimentally established for plant CLC homologues (Stockbridge et al., 2012; Last et al., 2018).

2.2.4 Fluoride coordination

Each CLC^F subunit binds two F^- ions at the canonical anion-binding sites designated as Fcen (central) and Fext (external) and both sites are simultaneously occupied in the wild-type structure (Last et al., 2018; McIlwain et al., 2021). Fext is coordinated primarily by backbone amides from residues G116–G119 at a helical break, together with the positive helix dipoles from the N-termini of αF and αN, and the sidechain hydroxyl of T320 hovers approximately 4 Å from the ion (Last et al., 2018).

While, Fcen is more elaborately coordinated by five to six ligands reflecting the high charge density of F^-. The conserved tyrosine Y396 contributes both its hydroxyl group and an edge-on aromatic quadrupolar interaction — an electropositive interaction with the π-system that is reprised in Fluc F- channels (Last et al., 2018). Critically, the conserved serine that coordinates Cl^- in conventional CLCs is absent in CLC^F and replaced by Met79, whose terminal methyl and γ-methylene groups polarized by the adjacent δ-sulfur contact Fcen directly (Last et al., 2018;

McIlwain et al., 2021). This methionine-mediated coordination is a key determinant of F^-/Cl^- selectivity showing the consistency with the hard-soft acid-base principle where F^-, a hard base is coordinated by a polarizable soft-acid-like moiety (McIlwain et al., 2021). Fcen coordination involves two additional residues that lack equivalents in Cl^--transporting CLCs: the hydroxyl group of T320 and E318. The carboxyl group of E318 is positioned 3.3 Å from the ion and likely acts as a protonated hydrogen-bond donor. (Last et al., 2018). The gating glutamate E118 serves as the proton carrier that cycles between Up and Down rotamers to alternately deliver H^+ from the extracellular milieu and release it to the cytoplasm, while F^- ions occupy the binding sites simultaneously (Last et al., 2018; McIlwain et al., 2021).

2.2.5 Fluoride Permeation and Transport Mechanism by CLCF Antiporters

The F^- transport cycle of CLC^F is propelled by the rotameric movements of the gating glutamate E118. This residue oscillates between Up and Down orientations to provide entrance to ion pathways from either side of the membrane (Last et al., 2018). The cycle starts with both Fcen and Fext binding sites occupied and E118 protonated in the Up position, where the extracellular proton pathway is open but the F^- ions are accessible only from the intracellular side (Last et al., 2018). The transfer of a proton to the cytoplasm is achieved through a clockwise and almost barrier-free rotation of protonated E118 into the Down position. This movement simultaneously displaces Fcen, which is subsequently released into the intracellular solution as HF with the assistance of protonated E318 (Chon et al., 2024). Deprotonated E118 upon vacation of the central binding site continues its clockwise movement along the anion pathway. This action results in the ejection of Fext from the external site, sending it into the extracellular vestibule (Chon et al., 2024). The external binding site, now occupied by the E118 carboxylate is subsequently reacquired by an incoming F- ion from the intracellular side by displacing E118 which in turn immediately accepts a proton from R117 and thereby reset the transporter for the next cycle (Chon et al., 2024). Competition between F^- and the negatively charged carboxylate of E118 for the external binding site is thus the central mechanistic driver (McIlwain et al., 2021; Chon et al., 2024). Molecular dynamics simulations studies further revealed that only a single F- ion occupies the transport pathway at any moment rather than the two seen in crystal structures further rationalizing the unique 1:1 F^-/H^+ stoichiometry (Mills et al., 2023; Chon et al., 2024). The proton and anion routes stay mostly distinct during the cycle, with access to the intracellular and extracellular environments alternating solely via E118 rotation, rather than through major structural rearrangements of the protein's primary chain (Chon et al., 2024).

While FEX transporters serve as the primary plasma membrane efflux mechanism for maintaining F- tolerance in plants, research suggests that other transporters also contribute to this physiological fate. For instance, CLC homologs in *Arabidopsis thaliana* have been reported to facilitate diverse functions including vacuolar storage, stomatal regulation, vesicular trafficking, and photosynthetic regulation. The tonoplast localized $2NO_3^-/1H^+$ antiporters AtCLCa and AtCLCb which use proton gradient generated by vacuolar H^+-ATPases to actively pump nitrate into the vacuole for massive storage, buffering the plant against nitrogen starvation (De Angeli et al., 2006). Another tonoplast localized AtCLCc, a Cl^-/H^+ antiporter that is heavily involved in regulating turgor pressure in guard cells, coordinating the opening and closing of stomata in response to environmental stress (Jossier et al., 2010).
The trans-Golgi network (TGN) localized *At*CLCd and *At*CLCf homologs are primarily associated with vesicular trafficking. By facilitating Cl^-/H^+ counter-transport, these proteins serve as critical

regulators of luminal pH within the Golgi apparatus, a process essential for effective protein sorting and the synthesis of cell wall components (von der Fecht-Bartenbach et al., 2007; Marmagne et al., 2007)
Furthermore, *At*CLCe is localized to the thylakoid membrane of chloroplasts, where it participates in photosynthetic regulation. It governs Cl^- flux during light-harvesting reactions, thereby maintaining the electrochemical equilibrium required for optimized photosynthetic electron transport (Marmagne et al., 2007; Herdean et al., 2016).

Investigating plant CLC homologues as F^- efflux mechanisms, analogous to bacterial CLC^F F^-/H^+ antiporters, is a necessary and interesting research frontier. These proteins may represent novel detoxification transporters in plants. Utilizing the proton motive force to actively expel cytoplasmic F^- they could substantially complement the overall established FEX channel mechanism.

2.3 ABC transporters

ATP-binding cassette (ABC) transporters represent one of the most biologically abundant and evolutionarily conserved superfamilies of integral membrane proteins with members identified across all kingdoms of life from bacteria to humans (Kang et al., 2011). The plant genome encodes for more than 100 ABC transporters, largely exceeding that of other organisms. In the model plant *Arabidopsis thaliana*, approximately 130 ABC transporter genes have been identified but only a small fraction of 22 genes have undergone comprehensive functional characterization (Kang et al., 2011). Furthermore, genome-wide analysis in the F^- hyperaccumulator plant *Camellia sinensis* have revealed over 900 putative ABC transporter genes, representing a diversity that underscores their fundamental roles across all physiological and biochemical processes in plants (Luo et al., 2022). The superfamily of ABC transporters is systematically classified into eight subfamilies (ABCA through ABCH), each differentiated by sequence homology and domain architecture, yet all share a conserved core structural blueprint (Kang et al., 2011; Luo et al., 2022). These integral membrane proteins work primarily as ATP-driven pumps, typically comprised of two transmembrane domains (TMDs) that form the membrane-spanning pore and two cytosolic nucleotide-binding domains (NBDs) carrying the conserved *Walker A and B motifs* responsible for ATP hydrolysis (Kang et al., 2011). The energy obtained from ATP binding and hydrolysis drives the active translocation of substrates across biological membranes, making these transporters to function as both exporters and importers depending on the organism and cellular context (Kang et al., 2011; Luo et al., 2022) (Figure 10). In eukaryotic systems, ABC transporters exhibit considerable structural diversity such as full-size transporters which encode all four domains within a single polypeptide, while half-size transporters dimerize to form functional units, and some subfamilies display either a forward (TMD-NBD) or reverse (NBD-TMD) domain organization (Kang et al., 2011). Although ABC transporters were originally identified for their roles in cellular detoxification through the vacuolar sequestration of xenobiotics and heavy metal conjugates, subsequent research has revealed that ABC transporters participate in a far broader spectrum of physiological processes (Kang et al., 2011). For instance, the ABCC subfamily is central to cellular detoxification wherein, tonoplast localized AtABCC1 and AtABCC2 mediate the vacuolar sequestration of phytochelatin-complexed heavy metals, conferring tolerance to Cd, mercury, and As. Also, mitochondria-localized AtABCB25 contributes to Fe-S cluster biogenesis and Cd tolerance (Kang et al., 2011). AtABCI16 and AtABCI17 confer Al tolerance (Kang et al.,

2011), while the soluble ABCE and ABCF subfamilies participate in ribosome recycling and translational control independent of transmembrane transport (Kang et al., 2011). Together, this superfamily underscores that ABC transporters in *Arabidopsis* are indispensable coordinators of heavy metal detoxification, phytohormone signaling, surface barrier formation, and nutritional homeostasis (Kang et al., 2011).

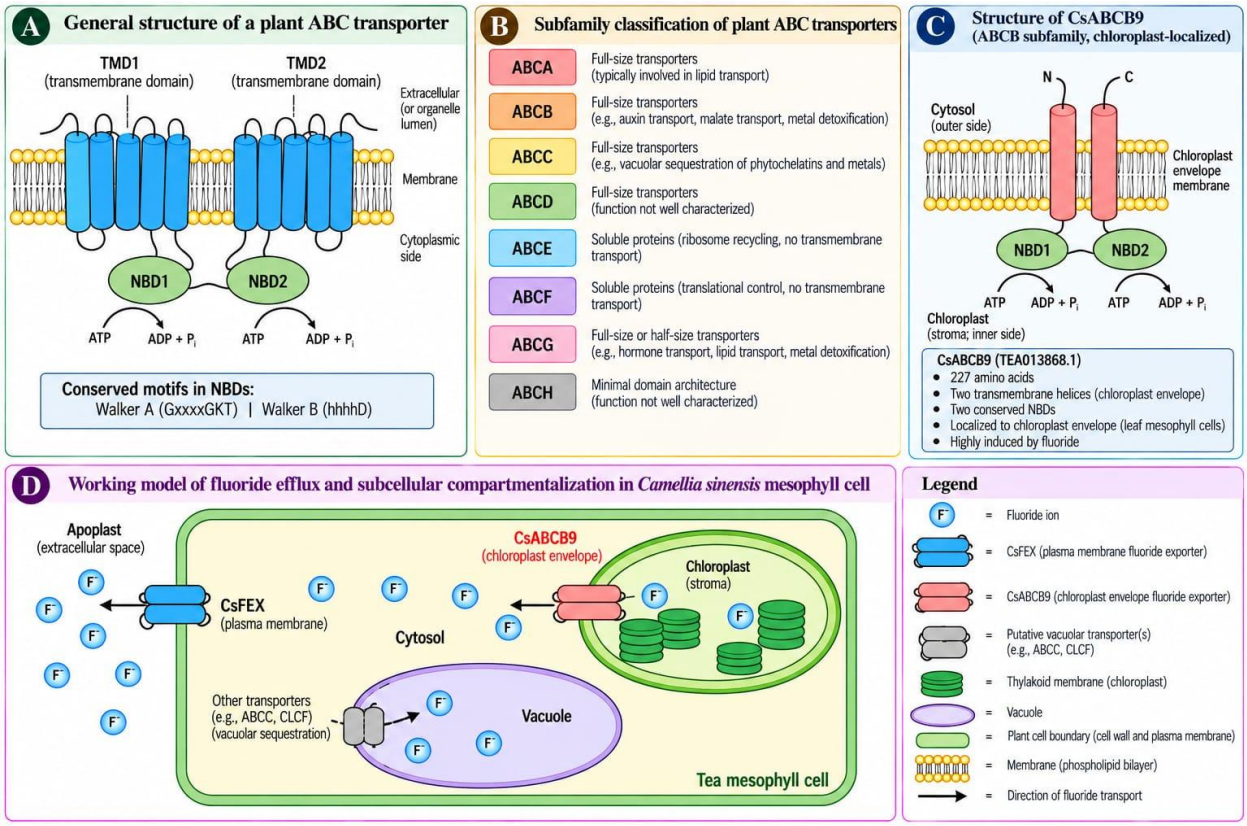


Figure 10. Structural organization and proposed role of ABC transporters in F^-homeostasis in plants. (A) General architecture of a membrane-bound ABC transporter comprising two transmembrane domains (TMDs) and two cytosolic nucleotide-binding domains (NBDs) involved in ATP hydrolysis. (B) Classification of ABC transporters into eight subfamilies (ABCA–ABCH) based on sequence homology and domain organization. (C) Predicted membrane topology and chloroplast-associated localization of CsABCB9 (TEA013868.1), a F^--responsive ABCB protein. (D) Proposed model of F^- compartmentalization in mesophyll cells, illustrating CsFEX-mediated F^- export across the plasma membrane, the putative involvement of CsABCB9 in chloroplast F^- redistribution, and unidentified tonoplast transporters potentially contributing to vacuolar sequestration. Solid arrows represent functionally supported F-export, whereas proposed intracellular transport routes remain hypothetical (Kang et al., 2011; Luo et al., 2022).

Within the diverse range of ABC transporters there is a functionally unique member that mediates the active efflux of toxic F^- ions effectively and this physiological mechanism has been most comprehensively characterized in the tea plant. Transcriptomic profiling of F^--treated *C. sinensis* leaves revealed that the ABC transporter of B subfamily is the most abundant and the gene CL667 (TEA013868.1) was found to exhibit a 3.89-fold upregulation under NaF stress, encoding an ABC subfamily B member 9 that was subsequently named CsABCB9 (Luo et al., 2022). Genetically, the *CsABCB9* open reading frame(ORF) spans 684 bp encoding a 227-amino-acid polypeptide with an anticipated secondary structure comprising 35.68% alpha-helix, 16.74% extended strand,

5.73% beta-turn, and 41.85% random coil (Luo et al., 2022). Structural modeling by SMART and TMHMM confirmed that CsABCB9 contains both conserved NBDs and TMDs with two transmembrane helices anchoring the protein in the chloroplast membrane (Luo et al., 2022). The expression of CsABCB9 is leaf-specific and highly induced by exogenous F^- correlating directly with F^- concentration in mesophyll cells (Luo et al., 2022). The Subcellular localization studies using CsABCB9 with eGFP fusions in *Nicotiana benthamiana* revealed that the protein present exclusively in the chloroplast envelope (Luo et al., 2022). The functional mechanism of F^- efflux was established through heterologous overexpression of CsABCB9 in *Escherichia coli* which significantly increased F^- resistance and lowered intracellular F^- content in similar fashion as CsFEX. Also, injection of CsABCB9 cRNA into *Xenopus laevis* oocytes similarly suppressed intracellular F^- accumulation (Luo et al., 2022). In another heterologous system of transgenic *Arabidopsis*, CsABCB9 overexpression conferred increased resistance to external F^-, consequently increased chlorophyll, xanthophyll, and soluble sugar concentrations compared to wild-type plants under F^- stress (Luo et al., 2022). This further elucidate an emergence of comprehensive working model under F^- stress wherein, increased cytosolic F^- is sensed by mesophyll cells which upregulate both CsABCB9 and the plasma membrane-localized CsFEX, consequently CsABCB9 actively exports F^- from the chloroplast lumen into the cytosol thereby protecting the photosynthetic apparatus from F^--induced thylakoid disruption and chlorophyll degradation, after which CsFEX exports F^- from the cytoplasmic matrix into the apoplastic space while few additional unknown vacuolar transporters sequester excess F^- away from sensitive organelles (Luo et al., 2022). This multifold efflux strategy is further supported by the ABC transporter CsCL667 (A-G subfamily member) and the anion-selective CLC^F protein both of which participate in transmembrane F^- flux and detoxification in a synergistic network (Yang et al., 2024).

The functional characterization of ABC transporters such as CsABCB9 and CsCL667 in F^- efflux alongside CLC^F and FEX proteins reveals a coordinated transporter network that facilitates F^- tolerance in hyperaccumulating plants (Yang et al., 2024). Future research objectives must prioritize the molecular investigation of the regulatory elements governing these transporter networks alongside the identification of novel transporter proteins responsible for F^- sequestration.

2.4 ALMT Transporters

The aluminum-activated malate transporter (ALMT) family belongs to a group of anion-permeable channel proteins that facilitate the transport of organic acids and inorganic anions across cellular membranes. Foundational studies established that ALMTs, such as TaALMT1 in *Triticum aestivum* and AtALMT1 in *Arabidopsis*, are plasma membrane-localized channels that facilitate the efflux of malate in response to Al^{3+}, thereby chelating the toxic cation in the rhizosphere (Barbier-Brygoo et al., 2011; Wang et al., 2022; Li et al., 2024). Since the foundational characterization of the ALMT family's pioneering role in *Triticum aestivum* and *Arabidopsis*, research has transitioned beyond mere stress mediation to elucidate further implications for diverse physiological roles. These include the regulation of stomatal dynamics, maintenance of cellular anion homeostasis, coordination of seed development, and the modulation of metabolic accumulation in fruits ((Barbier-Brygoo et al., 2011; Li et al., 2025). Members like AtALMT9 functions as a tonoplast-localized malate-activated chloride channel involved in stomatal opening while, AtALMT12 contributes to rapid-type anion currents in guard cells during abscisic acid-induced stomatal closure (Barbier-Brygoo et al., 2011). Also, other homologues such as MdALMT9 and SlALMT9 are known to govern malic acid accumulation in apple and tomato

fruits, respectively (Li et al., 2025). This functional pleiotropy has developed from the capacity of ALMT proteins to transport multiple anionic substrates, including malate, chloride, nitrate, and sulfate, based on cellular context and regulatory inputs (Li et al., 2024; Li et al., 2025).

In the recent studies of F^- hyperaccumulator *Camellia sinensis*, the aluminum-activated malate transporter (ALMT) family has recently been identified as a critical molecular coordinator in the physiological mechanism of F- tolerance (Li et al., 2025). Through recent, transcriptome-wide association studies(TWAS) and genome-wide identification, CsALMT6 and CsALMT14 were identified as candidate genes associated with differential F^- accumulation among tea cultivars (Li et al., 2024; Li et al., 2025). Here, CsALMT6 shows high transcript abundance in mature and old leaves which act as the primary sites of F^- deposition and its expression is significantly upregulated under F^- stress in both low-F^- and high-F^- cultivars. Also, the Heterologous expression of CsALMT6 in *Saccharomyces cerevisiae*, *Arabidopsis thaliana*, and *Populus* consistently improves F^- tolerance while reducing cellular F^- content, suggesting that CsALMT6 functions as a plasma membrane-localized anion channel mediating F^- efflux (Li et al., 2025). Notably, virus-induced gene silencing(VIGS) of CsALMT6 in tea plants resulted in increased F^- accumulation without changing the expression of traditional F^- exporters CsFEX1 and CsFEX2, indicating that CsALMT6 function independently of the established FEX-mediated detoxification pathway. Furthermore, CsALMT6 silencing significantly upregulated CsALMT9, implying potential functional redundancy or compensatory regulation within the ALMT family (Li et al., 2025).

Similarly, CsALMT14 has been involved in F^- tolerance through integrated metabolomic and transcriptomic analyses. Under F^- stress, integrated metabolomic and transcriptomic analyses identified malic and citric acids as key differentially accumulated metabolites, while weighted gene co-expression network analysis (WGCNA) positioned *Cs*ALMT14 as a central hub gene within a regulatory module highly enriched for transmembrane transporter activity (Li et al., 2025). Subcellular localization confirmed that CsALMT14 is present at the plasma membrane, and its heterologous expression in yeast and *Arabidopsis* conferred F^- tolerance linked with reduced F^- accumulation. Silencing CsALMT14 in tea plants by exploiting antisense oligonucleotides and virus-induced gene silencing led to decreased malic acid content, increased citric acid accumulation, and downregulation of malic acid biosynthesis-related genes (CsPEPC2, CsPEPC14, CsME2, CsME5, CsME16) alongside a citric acid degradation gene (CsGAD3)(Li et al., 2025). These observations suggest that CsALMT14 may regulate F^- tolerance not only through direct anion efflux but also by influencing organic acid metabolism, potentially via malate-mediated regulation of channel activity or through indirect effects on carbon flux. However, the precise molecular link between CsALMT14 and altered organic acid profiles remains to be elucidated.

Comparison of CsALMT6 and CsALMT14 with characterized ALMTs from other species, emerges several distinctive features. Unlike TaALMT1, which is activated by extracellular Al^{3+}, neither CsALMT6 nor CsALMT14 has been demonstrated to respond to aluminum which suggests that their primary substrate may be F^- or that they possess broader anion selectivity. This further aligns with observations that AtALMT9 and AtALMT12 are activated by malate rather than aluminum indicating that transactivation by permeant anions is a conserved regulatory mechanism within the family (Barbier-Brygoo et al., 2011). The ability of CsALMT6 and CsALMT14 to reduce F^- accumulation when overexpressed in heterologous systems and their occurrence on

plasma membrane supports a model in which these channels facilitate direct F^- efflux from the cytosol to the apoplast, thereby lowering cytoplasmic F^- concentrations and mitigating toxicity. Nevertheless, direct electrophysiological evidence demonstrating F^- permeation through CsALMT6 or CsALMT14 is currently lacking and the possibility that these transporters mediate F^--stimulated organic acid efflux, as observed for malate activation of R-type channels, cannot be excluded.

2.4.1 Structural detail of ALMT channels

Structural Insights into CsALMT6 and CsALMT14: Predictive Modeling Based on Conserved ALMT Architecture

High-resolution structural studies of CsALMT6 and CsALMT14 transporters are still a subject of experimentation. However, the recent available studies of cryo-electron microscopy structures for AtALMT1 (Wang et al., 2021), AtALMT9 (Lee et al., 2025), and GmALMT12 (Qin et al., 2022) provides a strong scheme for predicting the three-dimensional architecture of these tea plant transporters with reasonable rationale. Phylogenetic analysis attributes CsALMT6 within subfamily B of the ALMT family, while CsALMT14 belongs to a distinct clade, suggesting that both proteins likely adopt the usual homodimeric assembly characteristic of all structurally characterized ALMTs (Li et al., 2024; Li et al., 2025). On the basis of conserved topology established for AtALMT1 and AtALMT9, each CsALMT6 and CsALMT14 subunit is supposed to contain six N-terminal transmembrane helices (TM1–TM6), wherein TM2 and TM5 forming the pore-lining helices at the dimer interface, while TM1, TM3, TM4, and TM6 occupy peripheral positions. An internal structural repeat that relates TM1–TM3 and TM4–TM6 via a pseudo-two-fold axis parallel to the membrane is likely preserved, despite the low sequence identity seen between these repeats. Subsequent to the TM6 segment, a cytosolic domain consisting of six α-helices (H1–H6) is proposed to facilitate dimer stabilization through a network of hydrophobic interactions, salt bridges, and hydrogen bonding, orienting with the structural standards established for *At*ALMT1 (Wang et al., 2021).

Since, both CsALMT6 and CsALMT14 have been functionally associated with F^- efflux and localize to the plasma membrane, it may be presumed that their pore architecture might share features with both AtALMT1 and AtALMT9. The ion conduction pathway is probably a funnel-shaped channel which opens toward the cytosol with multiple positively charged residues mediating anion transport. Two pairs of highly conserved arginine residues, equivalent to Arg80 and Arg165 in AtALMT1 (Wang et al., 2021) are predicted to project into the pore center, where they coordinate anion binding through electrostatic interactions. Sequence alignments assays of CsALMTs indeed reveal the occurrence of these conserved arginine residues, suggesting their essential role in anion recognition and transport.

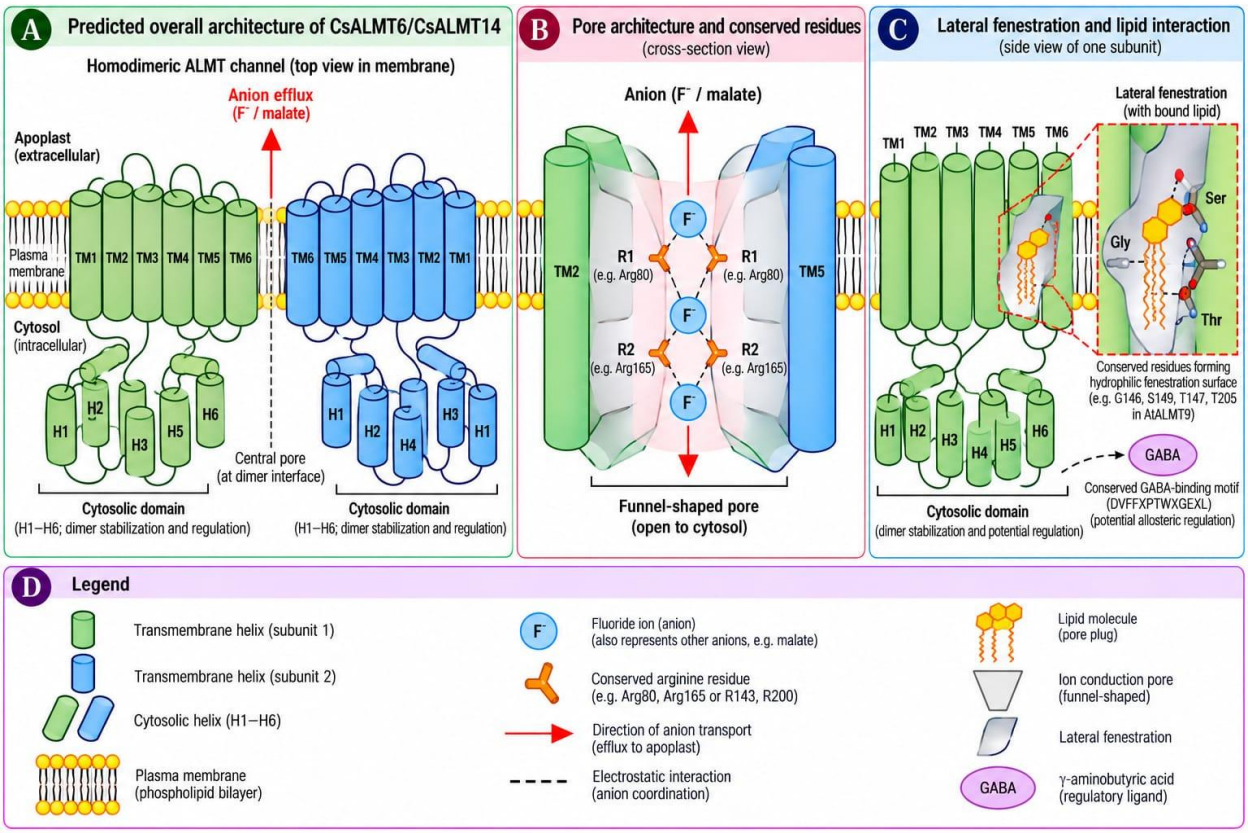


Figure 11. Predicted structural organization and regulatory features of CsALMT6 and CsALMT14 in plant. (A) Proposed homodimeric architecture comprising six transmembrane helices (TM1–TM6) and a cytosolic helical domain (H1–H6) per subunit. (B) Putative anion-conduction pathway highlighting conserved arginine residues potentially involved in substrate coordination. (C) Proposed lipid-interacting lateral fenestration and potential GABA-mediated regulation, inferred from structurally characterized ALMT homologues. These features remain predictive, and direct F- transport through CsALMT6 and CsALMT14 has not been experimentally established (Wang et al., 2021; Qin et al., 2022; Lee et al., 2025)

Notably, AtALMT9 structures disclose the presence of lateral fenestrations, a kind of openings in each protomer that joins the membrane bilayer to the central ion conduction pathway, which accommodate phospholipid molecules that act as pore plugs (Lee et al., 2025). Provided that CsALMT6 and CsALMT14 belong to clades that may share functional similarities with AtALMT9, it is likely that these tea plant transporters also possess lateral fenestrations that allow lipid-mediated regulation. The hydrophilic surfaces within these fenestrations formed by the exposed main-chain atoms of glycine residues and hydroxyl groups of serine and threonine residues (e.g., G146, S149, T147, T205 in AtALMT9), are conserved in CsALMT6 and CsALMT14 based on multiple sequence alignments, suggesting that lipid binding and pore-plugging mechanisms may regulate their activity. The occurrence of a putative dicarboxylate-binding site, formed by highly conserved arginine pairs specifically R143 and R200 as identified in *At*ALMT9, with equivalent residues likely preserved in *Cs*ALMT6 and *Cs*ALMT14 are proposed to facilitate substrate recognition; here, the positively charged side chains serve to stabilize either malate or F^- anions through favorable electrostatic interactions.

The gating mechanism of CsALMT6 and CsALMT14 may involve conformational rearrangements of the TM1–TM2 and TM5–TM6 loops, analogous to the aluminum-induced opening observed in AtALMT1 (Wang et al., 2021). For F^- transport specifically, the smaller ionic radius of F^- compared to malate may inflict distinct selectivity requirements. It is plausible that the arginine residues lining the pore, although vital for the coordination of anions, could facilitate the movement of F^- through a comparable mechanism of electrostatic attraction, albeit involving a distinct coordination geometry. Additionally, the occurrence of a conserved GABA-binding motif (DVFFXPTWXGEXL) in CsALMT6 and CsALMT14, as identified in other ALMTs (Ramesh et al., 2018), suggests potential regulation by γ-aminobutyric acid which may modulate channel activity through allosteric mechanisms involving the cytosolic domain.

In summary, while direct experimental validation awaits, the available structural biology of ALMT homologs provides a compelling predictive framework for CsALMT6 and CsALMT14. Both transporters are expected to adopt a homodimeric six-transmembrane-helix architecture per subunit, with a single ion-conducting pore formed at the dimer interface, lined by conserved arginine residues, and potentially regulated by lipid interactions through lateral fenestrations. Future cryo-EM studies will be essential to confirm these predictions and to elucidate the specific structural determinants of F- selectivity and gating in these tea plant transporters.

2.4.2 Mechanistic status of CsALMT6 and CsALMT14 in F^- transport

CsALMT6 represents a vivid evidence-based model for F^- efflux. Functional assays across yeast, *Arabidopsis* and poplar established studies show that CsALMT6 expression in heterologous systems reduces tissue F^- content. Furthermore, silencing *CsALMT6* in tea plants reduces leaf F^- accumulation without affecting the primary CsFEX pathway which provides a distinct, parallel detoxification route. This is also supported by its plasma membrane localization and induction by F^- stress, suggesting an inducible vectorial export mechanism. Despite this physiological validation, key mechanistic details such as ion selectivity, voltage dependence, and whether it is a channel or coupled antiport still require clarification (Li et al., 2024).

In contrast, the characterization of CsALMT14 is profoundly inconsistent. Currently, CsALMT14 is devoid of all direct experimental evidence including heterologous expression data or electrophysiological recording. While bioinformatic analysis predicts a plasma membrane location and a distinctive basic isoelectric point (pI 8.98) providing, these *in silico* features are speculative. Crucially, *CsALMT14* transcript was neither identified in F^--related genomic studies nor responsive to F^- stress (Li et al., 2024). Therefore, its biological function and any proposed F^- efflux role remain completely unannotated which demands the urgent need for systematic functional assays across the ALMT family in *C. sinensis*.

Collectively, the emerging evidence positions CsALMT6 and CsALMT14 as promising candidates for enhancing F^- tolerance in plants. However, several knowledge gaps are still remaining. These include i) substrate specificity and gating mechanisms of these transporters require rigorous electrophysiological characterization to confirm direct F^- transport, ii) the apparent independence of CsALMT6 from the FEX pathway which raises questions about the existence of parallel or redundant detoxification systems, iii) the mechanistic basis for the observed alterations in malate and citrate metabolism upon CsALMT14 silencing that further demand investigation including nature of organic acids whether serve as signaling molecules or

cotransported substrates. Future research employing patch-clamp electrophysiology, heterologous expression in *Xenopus* oocytes, and structure-function analyses are required to delineate the molecular determinants of F^- selectivity and to clarify the interplay between ALMT-mediated anion transport and organic acid homeostasis.

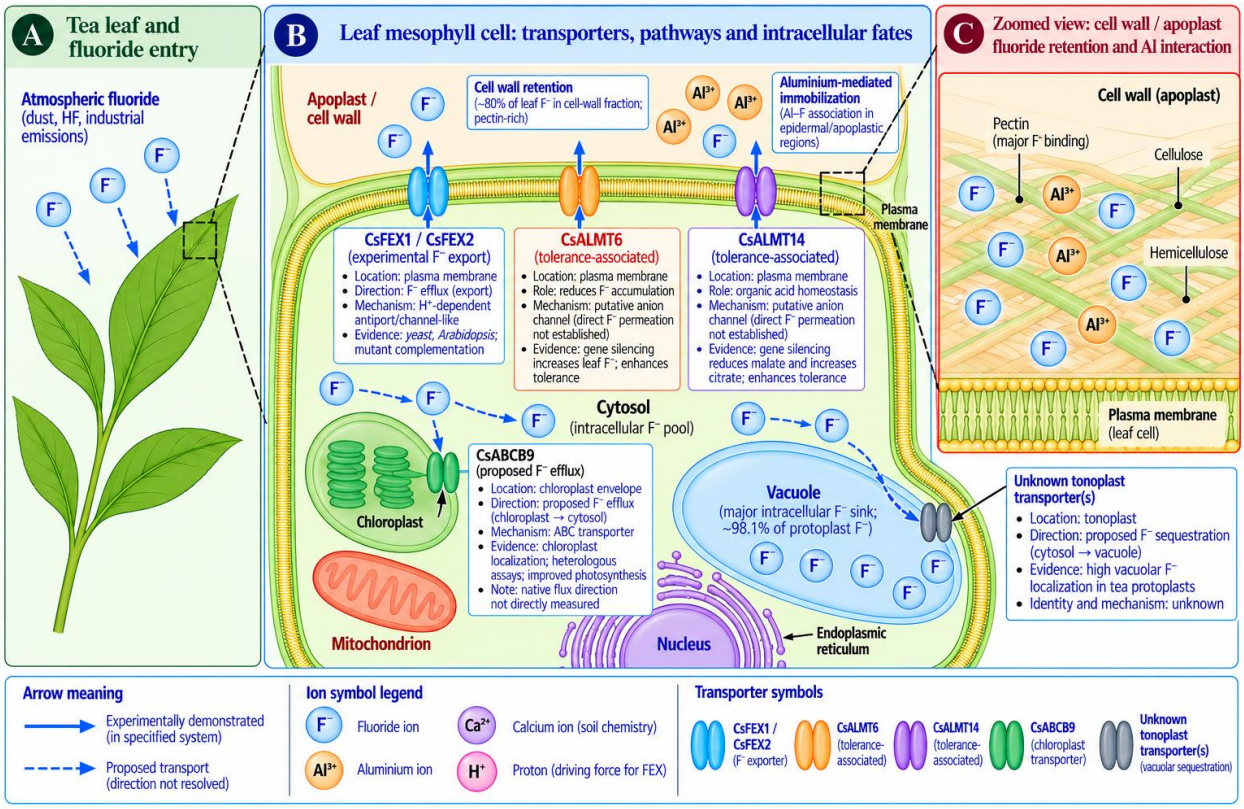


Figure 12. Schematic overview of F^- uptake, compartmentalization, and detoxification in tea (Camellia sinensis) leaf cells. (A) Atmospheric F^- deposition and foliar uptake, followed by its distribution within leaf tissues. (B) Fluoride homeostasis in mesophyll cells involves CsFEX1/CsFEX2-mediated efflux, tolerance-associated transporters CsALMT6 and CsALMT14, and putative CsABCB9-mediated chloroplast F- transport. Vacuolar sequestration through unidentified tonoplast transporters contributes to intracellular F- compartmentalization. (C) Fluoride retention within the pectin-rich cell wall and its association with aluminium may restrict cytosolic F- accumulation. Solid blue arrows indicate experimentally supported transport in specified systems, whereas dashed blue arrows represent proposed or unresolved transport pathways.

2.5 Nitrate Transporters (NRT)

Nitrate transporters (NRT) are the specialized membrane proteins present in the plants, algae and microorganisms to absorb and transport the NO_{3-} across cell membranes (Pu et al., 2023). According to the kinetic criteria, the NO_{3-} transport systems are classified as low-affinity transport system (LATS), inducible high-affinity transport system (iHATS), and constitutive high-affinity transport system (cHATS) (Glass et al., 1995; Crawford and Glass, 1998; Forde, 2000).

The NRT transporters belong to four main families: Nitrate transporter 1 (NRT1)/Peptide transporter (PTR) (NPF), Nitrate transporter 2 (NRT2), Chloride channel (CLC), and Slowly activating anion channel (SLAC)/SLAC-associated homologue (SLAH) (Leran et al., 2014; Orsel et al., 2002; Barbier-Brygoo et al., 2011; Wang et al., 2018; Vidal et al., 2020).
The structural studies predicted that NPF are composed of 12 transmembrane domains connected by short peptide loops and having a large hydrophilic loop between transmembrane domains 6 and 7 (Tsay et al., 2007). NPFs are widely distributed in both eukaryotes and prokaryotes and have been identified in various plant species. About 53 members of NPF family have been identified in *Arabidopsis thaliana* and around 93 members have been reported in Rice (Leran et al., 2014; von Wittgenstein et al., 2014).
In addition to this there is NAR1/FNT family of specialised transporters that regulates the transport of NO_{2-} and formate (HCO_2^-) in microbial and plant cell membranes (Lu et al., 2013; Wang et al., 2009). NRT2 proteins also anticipated to be composed of 12 α-helical transmembrane spans with a central cytoplasmic loop, relatively short in Arabidopsis compared with A. nidulans (Forde, 2000) and having variable hydrophilic N- and C-termini.

2.5.1 Subcellular locations of NRT transporters and their key functions

In most plants, three NRT2 transporters (NRT2.1, NRT2.2, NRT2.4) and two NRT1 transporters [NPF6.3 (NRT1.1/CHL1) and NPF4.6 (NRT1.2)] have been revealed as molecular components of root nitrate uptake (Tsay et al., 1993; Huang et al., 1999; Filleur et al., 2001; Kiba et al., 2012). All these five proteins localize onto the plasma membrane and their relative contribution depends on developmental stage and plant N status. All three NRT2 transporters are involved in HATS and NRT2.1 is the main HATS component under different conditions (Li et al., 2007). The NRT2.4 expression is subsequent to the high N starvation in plants, while NRT2.1 AND NRT2.2 expressed transiently during N starvation. NRT2.4 is polarised epidemally localized root transporter faces the vicinity of soil solution and demonstrate the high affinity for low NO_3^- availability (Kiba et al., 2012). The loss-of-function mutants of NRT2.4 shows insignificant growth phenotype under N-sufficient and N-limiting conditions and there is evidence that the triple mutants of NRT2.1, NRT2.2, and NRT2.4 produce less biomass under N limitation (Kiba et al., 2012). There also exist NO_3^- efflux mechanism in plants which is conferred by NPF2.7 (NAXT1), a plasma membrane-localized transporter in cortical root cells. NAXT1 loss-of-function mutants exhibit difficulty in NO_3^- excretion after medium acidification (Segonzac et al., 2007). NPF7.3 (NRT1.5) is a vascular transporter which expressed in pericycle cells surrounding the protoxylem and posses low-affinity bidirectional (influx–efflux) mechanism involved in loading nitrate into the xylem (Lin et al., 2008).

2.5.2 NRT transporter implicated in F^- influx

Traditionally, the NPF (NRT1/PTR) was involved in the transport of a variety of substrates from the rhizospheric soil solution via the root system, such as nitrates, nitrites, peptides, amino acids, phytohormones. Strikingly, in recent years the NPF transporters have also been implicated in

halide-managing plants, demonstrated by various homologues—ZmNPF6.4 (Wen et al., 2017), MtNPF6.5 (Xiao et al., 2021), AtNPF2.5 (Li et al., 2017), and VviNPF2.2 (Wu et al., 2022) in Cl^- transport. Similarly, one such homologue, CsNPF2.3, represents the first functionally characterized NPF member mediating F- transport in tea plant (Niu et al., 2025). The CsNPF2.3 transporter is encoded by TEA020860.1 and shares considerable sequence identity with AcNPF2.3 (76%) and the Cl^--efflux transporter VviNPF2.2 (57%) (Niu et al., 2025; Wu et al., 2022) that supports its placement within the NPF2 clade and invites structural and functional comparison with traditional NPF anion transporters (Corratgé-Faillie and Lacombe, 2017). The subcellular localisation of CsNPF2.3 onto the plasma membrane was confirmed by the GFP–AtPIP2A-mCherry colocalization (Niu et al., 2025; Nelson et al., 2007) and is predominantly expressed in roots, specifically in epidermal, cortex, and xylem parenchyma cells, with maximal signal in the cortex (Niu et al., 2025). The F^- transport activity was demonstrated by heterologous expression in yeast, revealing growth suppression and about 2–3-fold greater F^- accumulation at 0.1–0.5 mM without detecting NO_3^-, Cl^-, or Br^- transport under the assayed conditions (Niu et al., 2025). The overexpression in hairy roots resulted in higher F^- content in roots, stems, and leaves. The increased the leaf/root F ratio suggests improved translocation from roots to leaves (Niu et al., 2025). In the study across nine cultivars, root CsNPF2.3 expression showed positive correlations with root F ($r = 0.682$), leaf F^- ($r = 0.918$), and transport efficiency ($r = 0.911$) (Niu et al., 2025). In a manner dependent on concentration and time, F^- downregulated expression, aligning with a stress-responsive regulatory response (Niu et al., 2025). The role of CsNPF2.3 in mediating apoplastic F^- retrieval and soil-solution F^- uptake, which governs radial F^- movement toward the xylem is thus proposed (Niu et al., 2025; Barberon, 2016).

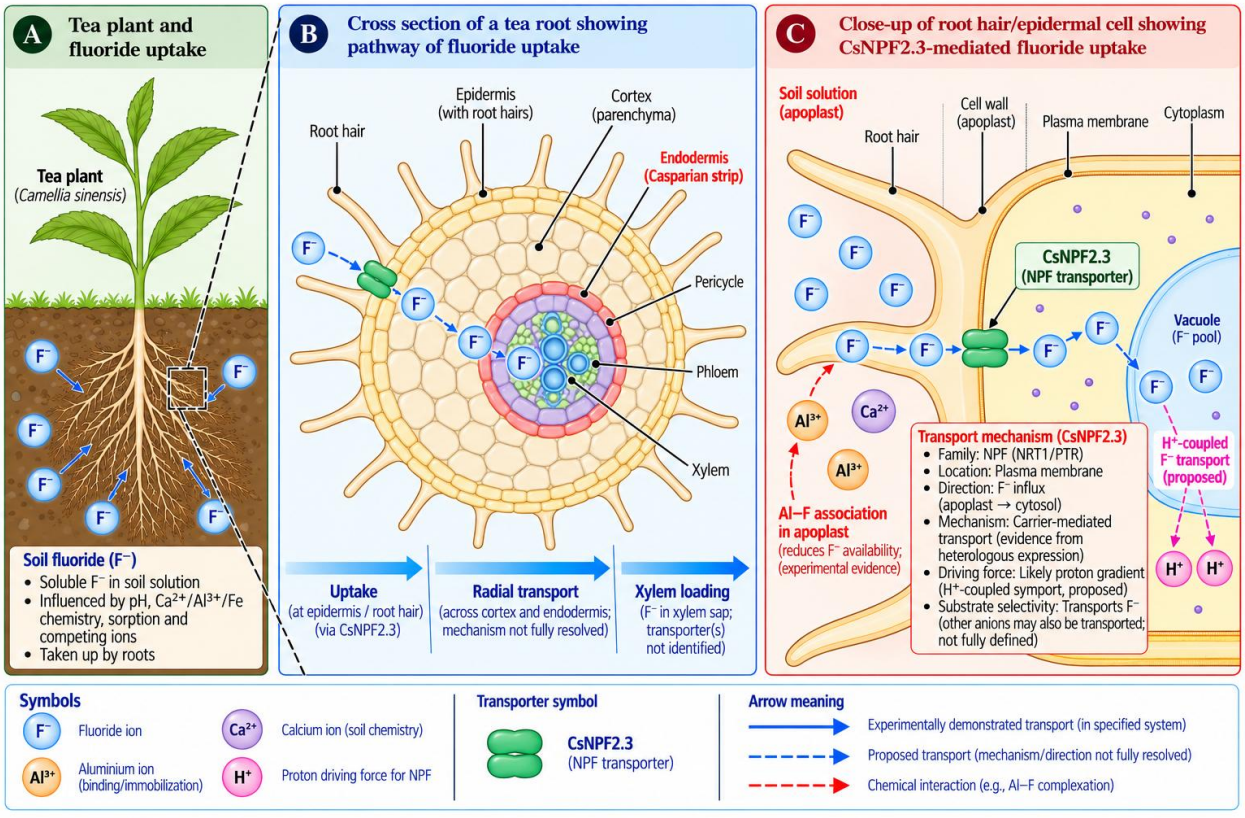


Figure 13. Proposed CsNPF2.3-mediated F^- uptake and transport in plant roots. (A) Uptake of soluble F^- from the soil solution by roots, influenced by soil pH, ionic composition, and metal–F- interactions. (B) Schematic root cross-section illustrating F^- influx across epidermal cells, followed by radial movement across the cortex and endodermis towards the vascular tissues for subsequent xylem loading. (C) Putative CsNPF2.3-mediated F^- influx across the root-hair plasma membrane, with possible proton-coupled transport and intracellular F^-accumulation. Aluminum–F- interactions may modulate F^- bioavailability in the apoplast. Solid blue arrows indicate experimentally supported transport in the specified system, dashed blue arrows denote proposed transport pathways, and dashed red arrows represent chemical interactions.

Conclusion

Fluoride contamination represents a growing environmental and public-health concern arising from natural mineral weathering and anthropogenic activities. Its mobility and bioavailability in soil–water systems are governed by pH, mineral composition, sorption dynamics, and metal–fluoride interactions, influencing groundwater contamination and plant exposure. At the cellular level, F^- disrupts essential biochemical processes through metal–fluoride complex formation, enzyme inhibition, ionic imbalance, and oxidative stress. In plants, these disturbances impair nutrient acquisition, membrane integrity, photosynthesis, stomatal regulation, and overall growth, highlighting the interconnected nature of F- -induced phytotoxicity. Understanding membrane-mediated F^- transport is therefore fundamental to elucidating plant F- tolerance. Among characterized transport systems, FEX proteins provide experimentally established mechanisms of selective F- efflux. Structural studies reveal distinct architectures of bacterial Fluc channels, comprising antiparallel dimers with two functional pores, and eukaryotic FEX exporters, possessing a nine-transmembrane architecture with one functional pore. Bacterial CLCF transporters additionally mediate coupled F^-/H^+ exchange, although analogous functions remain unverified in plants. Emerging evidence suggests potential involvement of additional transporter families, including CLC, ALMT, ABC, and NRT/NPF, in F- uptake, redistribution, and intracellular sequestration. Specifically, CsNPF2.3, CsALMT6, CsALMT14, and CsABCB9 represent promising candidates; however, their proposed F- -transport functions require direct experimental validation.

Future investigations should integrate structural biology, electrophysiology, heterologous expression, genetic manipulation, and spatially resolved F- profiling to establish transporter specificity, transport directionality, regulatory mechanisms, and physiological relevance. Particular attention should be directed towards identifying F- influx pathways, vacuolar sequestration mechanisms, and interactions between F- transport and nutrient homeostasis under environmentally relevant conditions. Ultimately, integrating environmental geochemistry with molecular transport mechanisms and whole-plant physiology will advance understanding of F- homeostasis and facilitate the development of F- -tolerant crops, reduced F- accumulation in edible tissues, and effective phytoremediation strategies for contaminated environments. These advances may strengthen sustainable agriculture and environmental risk mitigation.

REFERENCES

Accardi, A., & Miller, C. (2004). Secondary active transport mediated by a prokaryotic homologue of ClC Cl^- channels. *Nature*, *427*(6977), 803–807. https://doi.org/10.1038/nature02314

Accardi, A., Walden, M., Nguitragool, W., Jayaram, H., Williams, C., & Miller, C. (2005). Separate ion pathways in a CL−/H+ exchanger. *The Journal of General Physiology*, *126*(6), 563–570. https://doi.org/10.1085/jgp.200509417

Agarwal, S., Regon, P., Rehman, M., Tanti, B., & Panda, S. K. (2021). Genome-wide analysis of fluoride exporter genes in plants. *3 Biotech*, *11*(3), 124. https://doi.org/10.1007/s13205-021-02677-z

Ahmed, S.; Karamat, M.; Haider, A.; Jabeen, F.; Ahmad, M.N.; Ansari, M.; Zulfiqar, A.; Jalal, A.; Nizam, A. (2020) Ameliorative effects of salicylic acid on dry biomass and growth of Pisum sativum L. under sodium fluoride stress. Fluoride , 53, 335–355.

Baker, J. L., Sudarsan, N., Weinberg, Z., Roth, A., Stockbridge, R. B., & Breaker, R. R. (2011). Widespread genetic switches and toxicity resistance proteins for fluoride. *Science*, *335*(6065), 233–235. https://doi.org/10.1126/science.1215063

Banerjee, A., & Roychoudhury, A. (2019). Structural introspection of a putative fluoride transporter in plants. *3 Biotech*, *9*(3), 103. https://doi.org/10.1007/s13205-019-1629-4

Banerjee, A.; Roychoudhury, A. Fluorine: A biohazardous agent for plants and phyto remediation strategies for its removal from the environment. Biol. Plant. 2019, 63, 104–112.

Barberon, M. (2016). The endodermis as a checkpoint for nutrients. *New Phytologist*, *213*(4), 1604–1610. https://doi.org/10.1111/nph.14140

Barbier, O.; Arreola-Mendoza, L.; Del Razo, L.M. (2010) Molecular mechanisms of fluoride toxicity. Chem. Biol. Interact. , 188, 319–333.

Barbier-Brygoo, H., De Angeli, A., Filleur, S., Frachisse, J., Gambale, F., Thomine, S., & Wege, S. (2011). Anion Channels/Transporters in plants: From molecular bases to regulatory networks. *Annual Review of Plant Biology*, *62*(1), 25–51. https://doi.org/10.1146/annurev-arplant-042110-103741

Baunthiyal, M.; Ranghar, S. (2014) Physiological and biochemical responses of plants under fluoride stress: An overview. Fluoride ,47, 287–293.

Berbasova, T., Nallur, S., Sells, T., Smith, K. D., Gordon, P. B., Tausta, S. L., & Strobel, S. A. (2017). Fluoride export (FEX) proteins from fungi, plants and animals are “single barreled” channels containing one functional and one vestigial ion pore. *PLoS ONE*, *12*(5), e0177096. https://doi.org/10.1371/journal.pone.0177096

Berkowitz, D. B., Karukurichi, K. R., de la Salud-Bea, R., Nelson, D. L., & McCune, C. D. (2008). Use of Fluorinated Functionality in Enzyme Inhibitor Development: Mechanistic and Analytical Advantages. Journal of fluorine chemistry, 129(9), 731–742. https://doi.org/10.1016/j.jfluchem.2008.05.016.

Bhattacharya P, Claesson M, Bundschuh J, Sracek O, Fagerberg J, Jacks G, Martin RA, Storniolo A, Thir JM (2006) Distribution and mobility of arsenic in the Río Dulce alluvial aquifers in Santiago del Estero Province, Argentina. Sci Total Environ 358(1–3):97–120

Brammer, A. E., Stockbridge, R. B., & Miller, C. (2014). F−/Cl− selectivity in CLCF-type F−/H+ antiporters. *The Journal of General Physiology*, *144*(2), 129–136. https://doi.org/10.1085/jgp.201411225

Chen, Y., Wang, S., Nan, Z., Ma, J., Zang, F., Li, Y., & Zhang, Q. (2016). Effect of fluoride and cadmium stress on the uptake and translocation of fluoride and cadmium and other mineral nutrition elements in radish in single element or co-taminated sierozem. *Environmental and Experimental Botany*, *134*, 54–61. https://doi.org/10.1016/j.envexpbot.2016.11.002

Chon, N. L., & Lin, H. (2024). Fluoride Ion Binding and Translocation in the CLCF Fluoride/Proton Antiporter: Molecular Insights from Combined Quantum-Mechanical/Molecular-Mechanical Modeling. *The Journal of Physical Chemistry B*, *128*(11), 2697–2706. https://doi.org/10.1021/acs.jpcb.4c00079

Corratgé-Faillie, C., & Lacombe, B. (2017). Substrate (un)specificity of Arabidopsis NRT1/PTR FAMILY (NPF) proteins. *Journal of Experimental Botany*, *68*(12), 3107–3113. https://doi.org/10.1093/jxb/erw499

Crawford, N. M., & Glass, A. D. (1998). Molecular and physiological aspects of nitrate uptake in plants. *Trends in Plant Science*, *3*(10), 389–395. https://doi.org/10.1016/s1360-1385(98)01311-9

Cronk, Q., Ojeda, I., & Pennington, R. T. (2006). Legume comparative genomics: progress in phylogenetics and phylogenomics. *Current Opinion in Plant Biology*, *9*(2), 99–103. https://doi.org/10.1016/j.pbi.2006.01.011

Currell M, Cartwright I, Raveggi M, Han D (2011) Controls on elevated fluoride and arsenic concentrations in groundwater from the Yuncheng Basin, China. Appl Geochem 26(4):540–552

De Angeli, A., Monachello, D., Ephritikhine, G., Frachisse, J. M., Thomine, S., Gambale, F., & Barbier-Brygoo, H. (2006). The nitrate/proton antiporter AtCLCa mediates nitrate accumulation in plant vacuoles. *Nature*, *442*(7105), 939–942. https://doi.org/10.1038/nature05013

Doley, D.; Hill, R.J.; Riese, R.H. (2004) Environmental fluoride in Australasia: Ecological effects, regulation and management. Clean Air Environ. Qual. , 38, 35–55.

Dupuis, A., Issartel, J., & Vignais, P. V. (1989). Direct identification of the fluoroaluminate and fluoroberyllate species responsible for inhibition of the mitochondrial F1-ATPase. *FEBS Letters*, *255*(1), 47–52. https://doi.org/10.1016/0014-5793(89)81058-0

Dutzler, R., Campbell, E. B., & MacKinnon, R. (2003). Gating the selectivity filter in CLC chloride channels. *Science*, *300*(5616), 108–112. https://doi.org/10.1126/science.1082708

Dutzler, R., Campbell, E. B., Cadene, M., Chait, B. T., & MacKinnon, R. (2002). X-ray structure of a ClC chloride channel at 3.0 Å reveals the molecular basis of anion selectivity. *Nature*, *415*(6869), 287–294. https://doi.org/10.1038/415287a

Edmunds, W. M., & Smedley, P. L. (2012). Fluoride in natural waters. In *Springer eBooks* (pp. 311–336). https://doi.org/10.1007/978-94-007-4375-5_13

Eleftheriou, E.P.; Tsekos, I. (1991) Fluoride effects on leaf cell ultrastructure of olive trees growing in the vicinity of the aluminium factory of Greece. Trees , 5, 83–89.

Elloumi, N., Ben Abdallah, F., Mezghani, I., Rhouma, A., & Boukhris, M. (2005). Effect of fluoride on almond seedlings in culture solution. *Fluoride*, *38*(3), 193–198.

Elloumi, N., Zouari, M., Mezghani, I., Abdallah, F. B., Woodward, S., & Kallel, M. (2017). Adaptive biochemical and physiological responses of Eriobotrya japonica to fluoride air pollution. *Ecotoxicology*, *26*(7), 991–1001. https://doi.org/10.1007/s10646-017-1827-y

Emamjomeh, M.M.; Sivakumar, M. (2009) Fluoride removal by a continuous flow electrocoagulation reactor. J. Environ. Manag. , 90, 1204–1212.

Farooqi A, Masuda H, Firdous N (2007) Toxic fluoride and arsenic contaminated groundwater in the Lahore and Kasur Districts, Punjab, Pakistan and possible contaminant sources. Environ Pollut 145(3):839–849

Filleur, S., Dorbe, M., Cerezo, M., Orsel, M., Granier, F., Gojon, A., & Daniel-Vedele, F. (2001). An Arabidopsis T-DNA mutant affected in Nrt2 genes is impaired in nitrate uptake. *FEBS Letters*, *489*(2–3), 220–224. https://doi.org/10.1016/s0014-5793(01)02096-8

Forde, B. G. (2000). Nitrate transporters in plants: structure, function and regulation. *Biochimica Et Biophysica Acta (BBA) - Biomembranes*, *1465*(1–2), 219–235. https://doi.org/10.1016/s0005-2736(00)00140-1

Fornasiero, R.B. (2001) Phytotoxic effects of fluorides. Plant Sci. , 161, 979–985.

Gadi, B. R., Kumar, R., Goswami, B., Rankawat, R., & Rao, S. R. (2020). Recent Developments in Understanding Fluoride Accumulation, Toxicity, and Tolerance Mechanisms in Plants: an Overview. Journal of Soil Science and Plant Nutrition, 21(1), 209–228. https://doi.org/10.1007/s42729-020-00354-3

Ghosh, A., Mukherjee, K., Ghosh, S. K., & Saha, B. (2012). Sources and toxicity of fluoride in the environment. *Research on Chemical Intermediates*, *39*(7), 2881–2915. https://doi.org/10.1007/s11164-012-0841-1

Glass, A. D. M., and Siddiqi, M. Y. (1995). "Nitrogen absorption by plant roots," in Nitrogen Nutrition in Higher Plants. Ed. H. S. Srivastava and R. P. Singh (New Delhi, India: Associated Publishing Co.), pp. 21–56

Haddy, A.; Lee, I.; Shin, K.; Tai, H. (2018) Characterization of fluoride inhibition in photosystem II lacking extrinsic PsbP and PsbQ subunits. J. Photochem. Photobiol. B Biol., 185, 1–9.

Hata, S., Iwami, Y., Kamiyama, K., & Yamada, T. (1990a). Biochemical Mechanisms of Enhanced Inhibition of Fluoride on the Anaerobic Sugar Metabolism by Streptococcus sanguis. *Journal of Dental Research*, *69*(6), 1244–1247. https://doi.org/10.1177/00220345900690060401

Hata, S., Iwami, Y., Kamiyama, K., & Yamada, T. (1990b). Biochemical Mechanisms of Enhanced Inhibition of Fluoride on the Anaerobic Sugar Metabolism by Streptococcus sanguis. *Journal of Dental Research*, *69*(6), 1244–1247. https://doi.org/10.1177/00220345900690060401

Haydon, M. J., Román, Á., & Arshad, W. (2015). Nutrient homeostasis within the plant circadian network. Frontiers in Plant Science, 6, 299. https://doi.org/10.3389/fpls.2015.00299

Herdean, A., Nziengui, H., Zsiros, O., Solymosi, K., Garab, G., Lundin, B., & Spetea, C. (2016). The Arabidopsis thylakoid chloride Channel ATCLCE functions in chloride homeostasis and regulation of photosynthetic electron transport. *Frontiers in Plant Science*, *7*, 115. https://doi.org/10.3389/fpls.2016.00115

Huang, N., Liu, K., Lo, H., & Tsay, Y. (1999). Cloning and functional characterization of an arabidopsis nitrate transporter gene that encodes a constitutive component of Low-Affinity uptake. *The Plant Cell*, *11*(8), 1381–1392. https://doi.org/10.1105/tpc.11.8.1381

Jentsch, T. J., & Pusch, M. (2018). CLC Chloride Channels and Transporters: Structure, function, physiology, and disease. *Physiological Reviews*, *98*(3), 1493–1590. https://doi.org/10.1152/physrev.00047.2017

Ji, C., Stockbridge, R. B., & Miller, C. (2014). Bacterial fluoride resistance, Fluc channels, and the weak acid accumulation effect. *The Journal of General Physiology*, *144*(3), 257–261. https://doi.org/10.1085/jgp.201411243

Johnston, N. R., & Strobel, S. A. (2020). Principles of fluoride toxicity and the cellular response: a review. Archives of toxicology, 94(4), 1051–1069. https://doi.org/10.1007/s00204-020-02687-5

Jossier, M., Kroniewicz, L., Dalmas, F., Thiec, D. L., Ephritikhine, G., Thomine, S., Barbier-Brygoo, H., Vavasseur, A., Filleur, S., & Leonhardt, N. (2010). The Arabidopsis vacuolar anion transporter, AtCLCc, is involved in the regulation of stomatal movements and contributes to salt tolerance. *The Plant Journal*, *64*(4), 563–576. https://doi.org/10.1111/j.1365-313x.2010.04352.x

Junior, A.M.D.; Oliva, M.A.; Martinez, C.A.; Cambraia, J. (2007) Effects of fluoride emissions on two tropical grasses: Chloris gayana and Panicum maximum cv. Colonião. Ecotoxicol. Environ. Saf. , 67, 247–253.

Kamiński, J., Stachelska-Wierzchowska, A., Michalczyk, D. J., Klimkowicz-Pawlas, A., Olkowska, E., Wolska, L., & Piotrowicz-Cieślak, A. I. (2024). Changes in Metabolism and Content of Chlorophyll in Common Duckweed (Lemna minor L.) Caused by Environmental Contamination with Fluorides. *Molecules*, *29*(10), 2336. https://doi.org/10.3390/molecules29102336

Kang, C., An, M., Heidari, S., Torabifard, H., Ohi, M. D., & Stockbridge, R. B. (2025). The molecular mechanism of fluoride export by the eukaryotic fluoride channel FEX. *Nature Communications*, *17*(1), 589. https://doi.org/10.1038/s41467-025-67289-0

Kang, J., Park, J., Choi, H., Burla, B., Kretzschmar, T., Lee, Y., & Martinoia, E. (2011). Plant ABC transporters. *The Arabidopsis Book*, *9*, e0153. https://doi.org/10.1199/tab.0153

Kiba, T., Feria-Bourrellier, A., Lafouge, F., Lezhneva, L., Boutet-Mercey, S., Orsel, M., Bréhaut, V., Miller, A., Daniel-Vedele, F., Sakakibara, H., & Krapp, A. (2012). The Arabidopsis nitrate transporter NRT2.4 plays a double role in roots and shoots of Nitrogen-Starved plants. *The Plant Cell*, *24*(1), 245–258. https://doi.org/10.1105/tpc.111.092221

Kumar, R., Sinha, R., Sharma, P. K., Ivy, N., Kumar, P., Kant, N., Jha, A., Jha, P. K., Gupta, P. K., Sharma, P., Singh, R. K., Singh, R. P., Ghosh, A., & Prasad, P. V. V. (2021). Bioaccumulation of fluoride in plants and its microbially assisted remediation: A review of biological processes and technological performance. *Processes*, *9*(12), 2154. https://doi.org/10.3390/pr9122154

Last NB, Kolmakova-Partensky L, Shane T, Miller C. Mechanistic signs of double-barreled structure in a fluoride ion channel. Elife. 2016 Jul 23;5:e18767. doi: 10.7554/eLife.18767. PMID: 27449280; PMCID: PMC4969038

Last, N. B., Stockbridge, R. B., Wilson, A. E., Shane, T., Kolmakova-Partensky, L., Koide, A., Koide, S., & Miller, C. (2018). A CLC-type F-/H+ antiporter in ion-swapped conformations. *Nature Structural & Molecular Biology*, *25*(7), 601–606. https://doi.org/10.1038/s41594-018-0082-0

Lee, Y., Demes-Causse, E., Yoo, J., Jang, S. Y., Jung, S., Jaślan, J., Hwang, G., Yoo, J., De Angeli, A., & Lee, S. (2025). Structural basis for malate-driven, pore lipid-regulated activation of the Arabidopsis vacuolar anion channel ALMT9. *Nature Communications*, *16*(1), 1817. https://doi.org/10.1038/s41467-025-56940-5

Léran, S., Varala, K., Boyer, J., Chiurazzi, M., Crawford, N., Daniel-Vedele, F., David, L., Dickstein, R., Fernandez, E., Forde, B., Gassmann, W., Geiger, D., Gojon, A., Gong, J., Halkier, B. A., Harris, J. M., Hedrich, R., Limami, A. M., Rentsch, D., . . . Lacombe, B. (2014). A unified nomenclature of NITRATE TRANSPORTER 1/PEPTIDE TRANSPORTER family members in plants. *Trends in Plant Science*, *19*(1), 5–9. https://doi.org/10.1016/j.tplants.2013.08.008

Levy, A. A., & Feldman, M. (2022). Evolution and origin of bread wheat. *The Plant Cell*, *34*(7), 2549–2567. https://doi.org/10.1093/plcell/koac130

Li, B., Qiu, J., Jayakannan, M., Xu, B., Li, Y., Mayo, G. M., Tester, M., Gilliham, M., & Roy, S. J. (2017). AtNPF2.5 Modulates Chloride (Cl−) Efflux from Roots of Arabidopsis thaliana. *Frontiers in Plant Science*, *7*, 2013. https://doi.org/10.3389/fpls.2016.02013

Li, D., Jin, Y., Lu, Q., Ren, N., Zhang, X., Li, L., Hong, G., Chen, Q., Zhao, Y., Wang, Y., & Li, Q. (2025). Calmodulin1–Calmodulin Binding Transcription Activator (CAM1–CAMTA) negatively regulate the transcription of Fluoride Export Gene 1 (FEX1) to mediate fluoride transport in tea (Camellia sinensis). *Journal of Experimental Botany*, *76*(10), 2715–2726. https://doi.org/10.1093/jxb/eraf113

Li, H., Ma, X., Huang, X., Ji, W., Chen, K., Xu, S., & Gao, P. (2023). Fluoride contents in commonly used commercial phosphate fertilizers and their potential risks in China. *Environmental Monitoring and Assessment*, *195*(9), 1051. https://doi.org/10.1007/s10661-023-11623-w

Li, L. (2003). The Biochemistry and Physiology of Metallic fluoride: Action, mechanism, and implications. *Critical Reviews in Oral Biology & Medicine*, *14*(2), 100–114. https://doi.org/10.1177/154411130301400204

Li, Q., Zhang, R., Hu, X., Ni, D., Chen, Y., & Wang, M. (2024). Aluminum-activated malate transporter family member CsALMT6 mediates fluoride resistance in tea plants (Camellia sinensis). *Horticulture Research*, *12*(4), uhae353. https://doi.org/10.1093/hr/uhae353

Li, Q., Zhu, W., Yan, Z., Ni, D., Chen, Y., & Wang, M. (2025). Integrated metabolomics and transcriptomics analyses reveal aluminum-activated malate transporter CsALMT14 contributing to fluoride tolerance in F-hyperaccumulator Camellia sinensis. *Ecotoxicology and Environmental Safety*, *292*, 117932. https://doi.org/10.1016/j.ecoenv.2025.117932

Li, W., Wang, Y., Okamoto, M., Crawford, N. M., Siddiqi, M. Y., & Glass, A. D. (2007). Dissection of the ATNRT2.1 : ATNRT2.2 Inducible High-Affinity Nitrate Transporter Gene Cluster. *PLANT PHYSIOLOGY*, *143*(1), 425–433. https://doi.org/10.1104/pp.106.091223

Lim, H., Stockbridge, R. B., & Miller, C. (2013). Fluoride-dependent interruption of the transport cycle of a CLC Cl−/H+ antiporter. *Nature Chemical Biology*, *9*(11), 721–725. https://doi.org/10.1038/nchembio.1336

Lin, S., Kuo, H., Canivenc, G., Lin, C., Lepetit, M., Hsu, P., Tillard, P., Lin, H., Wang, Y., Tsai, C., Gojon, A., & Tsay, Y. (2008). Mutation of the Arabidopsis NRT1.5 nitrate transporter causes defective Root-to-Shoot nitrate transport. *The Plant Cell*, *20*(9), 2514–2528. https://doi.org/10.1105/tpc.108.060244

Lü, W., Du, J., Schwarzer, N. J., Wacker, T., Andrade, S. L., & Einsle, O. (2013). The formate/nitrite transporter family of anion channels. *Biological Chemistry*, *394*(6), 715–727. https://doi.org/10.1515/hsz-2012-0339

Luo, B., Guang, M., Yun, W., Ding, S., Ren, S., & Gao, H. (2022). Camellia sinensis Chloroplast Fluoride Efflux Gene CsABCB9 Is Involved in the Fluoride Tolerance Mechanism. *International Journal of Molecular Sciences*, *23*(14), 7756. https://doi.org/10.3390/ijms23147756

Luo, J.; Ni, D.; Li, C.; Du, Y.; Chen, Y. (2021) The relationship between fluoride accumulation in tea plant and changes in leaf cell wall structure and composition under different fluoride conditions. Environ. Pollut., 270, 116283.

Manoharan, V., Loganathan, P., Tillman, R., & Parfitt, R. (2006). Interactive effects of soil acidity and fluoride on soil solution aluminium chemistry and barley (Hordeum vulgare L.) root growth. *Environmental Pollution*, *145*(3), 778–786. https://doi.org/10.1016/j.envpol.2006.05.015

Marmagne, A., Vinauger-Douard, M., Monachello, D., De Longevialle, A. F., Charon, C., Allot, M., Rappaport, F., Wollman, F., Barbier-Brygoo, H., & Ephritikhine, G. (2007). Two members of the Arabidopsis CLC (chloride channel) family, AtCLCe and AtCLCf, are associated with thylakoid and Golgi membranes, respectively. *Journal of Experimental Botany*, *58*(12), 3385–3393. https://doi.org/10.1093/jxb/erm187

McCormick, N. E., & Jakeman, D. L. (2015). On the mechanism of phosphoenolpyruvate synthetase (PEPs) and its inhibition by sodium fluoride: potential magnesium and aluminum fluoride complexes of phosphoryl transfer. *Biochemistry and Cell Biology*, *93*(3), 236–240. https://doi.org/10.1139/bcb-2014-0153

McIlwain, B. C., Ruprecht, M. T., & Stockbridge, R. B. (2021). Membrane exporters of fluoride ion. *Annual Review of Biochemistry*, *90*(1), 559–579. https://doi.org/10.1146/annurev-biochem-071520-112507

Miles, R. D., Gorrell, A., & Ferry, J. G. (2002). Evidence for a Transition State Analog, MgADP-Aluminum Fluoride-Acetate, in Acetate Kinase from Methanosarcina thermophila. *Journal of Biological Chemistry*, *277*(25), 22547–22552. https://doi.org/10.1074/jbc.m105921200

Mills, K. R., & Torabifard, H. (2023). Uncovering the mechanism of the Proton-Coupled fluoride transport in the CLC F antiporter. *Journal of Chemical Information and Modeling*, *63*(8), 2445–2455. https://doi.org/10.1021/acs.jcim.2c01228

Nelson, B. K., Cai, X., & Nebenführ, A. (2007). A multicolored set of in vivo organelle markers for co-localization studies in Arabidopsis and other plants. *The Plant Journal*, *51*(6), 1126–1136. https://doi.org/10.1111/j.1365-313x.2007.03212.x

Niu, H., Wang, J., Liao, Z., Deng, Y., Chen, Q., Peng, C., Chen, G., Hou, R., Wan, X., Zhang, Z., & Cai, H. (2025). Root-specific expression of CsNPF2.3 is involved in modulating fluoride accumulation in tea plant (Camellia sinensis). *Horticulture Research*, *12*(6), uhaf072. https://doi.org/10.1093/hr/uhaf072

Nordstrom, D. K., & Jenne, E. A. (1977). Fluorite solubility equilibria in selected geothermal waters. *Geochimica Et Cosmochimica Acta*, *41*(2), 175–188. https://doi.org/10.1016/0016-7037(77)90224-1

Orsel, M., Krapp, A., & Daniel-Vedele, F. (2002). Analysis of the NRT2 nitrate transporter family in Arabidopsis. Structure and gene expression. *PLANT PHYSIOLOGY*, *129*(2), 886–896. https://doi.org/10.1104/pp.005280

Ozsvath, D. L. (2008). Fluoride and environmental health: a review. *Reviews in Environmental Science and Bio/Technology*, *8*(1), 59–79. https://doi.org/10.1007/s11157-008-9136-9

Panda, D. (2015) Fluoride toxicity stress: Physiological and biochemical consequences on plants. Int. J. Bio-Resour. Environ. Agric. Sci. , 1, 70–84.

Pellegrini, E., Juyoux, P., von Velsen, J., Baxter, N. J., Dannatt, H. R. W., Jin, Y., Cliff, M. J., Waltho, J. P., & Bowler, M. W. (2024). Metal fluorides-multi-functional tools for the study of phosphoryl transfer enzymes, a practical guide. Structure (London, England : 1993), 32(10), 1834–1846.e3. https://doi.org/10.1016/j.str.2024.07.007

Pickering, W. (1985). The mobility of soluble fluoride in soils. *Environmental Pollution Series B Chemical and Physical*, *9*(4), 281–308. https://doi.org/10.1016/0143-148x(85)90004-7

Picollo, A., Malvezzi, M., Houtman, J. C. D., & Accardi, A. (2009). Basis of substrate binding and conservation of selectivity in the CLC family of channels and transporters. *Nature Structural & Molecular Biology*, *16*(12), 1294–1301. https://doi.org/10.1038/nsmb.1704

Prabhu, S. M., Yusuf, M., Ahn, Y., Park, H. B., Choi, J., Amin, M. A., Yadav, K. K., & Jeon, B. (2023). Fluoride occurrence in environment, regulations, and remediation methods for soil: A comprehensive review. *Chemosphere*, *324*, 138334. https://doi.org/10.1016/j.chemosphere.2023.138334

Pu, Y., Wang, P., Abbas, M., Khan, M. A., Xu, J., Yang, Y., Zhou, T., Zheng, K., Chen, Q., & Sun, G. (2023). Genome-wide identification and analyses of cotton high-affinity nitrate transporter 2 family genes and their responses to stress. *Frontiers in Plant Science*, *14*, 1170048. https://doi.org/10.3389/fpls.2023.1170048

Qin, J., Chai, G., Brewer, J. M., Lovelace, L. L., & Lebioda, L. (2005). Fluoride inhibition of enolase: crystal structure and thermodynamics,. *Biochemistry*, *45*(3), 793–800. https://doi.org/10.1021/bi051558s

Qin, J., Chai, G., Brewer, J. M., Lovelace, L. L., & Lebioda, L. (2006). Fluoride inhibition of enolase: crystal structure and thermodynamics. Biochemistry, 45(3), 793–800. https://doi.org/10.1021/bi051558s

Qin, L., Tang, L., Xu, J., Zhang, X., Zhu, Y., Zhang, C., Wang, M., Liu, X., Li, F., Sun, F., Su, M., Zhai, Y., & Chen, Y. (2022). Cryo-EM structure and electrophysiological characterization of ALMT from Glycine max reveal a previously uncharacterized class of anion channels. *Science Advances*, *8*(9), eabm3238. https://doi.org/10.1126/sciadv.abm3238

Ramesh, S. A., Kamran, M., Sullivan, W., Chirkova, L., Okamoto, M., Degryse, F., McLaughlin, M., Gilliham, M., & Tyerman, S. D. (2018). Aluminum-Activated malate transporters can facilitate GABA transport. *The Plant Cell*, *30*(5), 1147–1164. https://doi.org/10.1105/tpc.17.00864

Reddy, M. P., & Kaur, M. (2007). Sodium Fluoride Induced Growth and Metabolic Changes in Salicornia brachiata Roxb. *Water Air & Soil Pollution*, *188*(1–4), 171–179. https://doi.org/10.1007/s11270-007-9533-7

Rhimi, N.; Mezghani, I.; Elloumi, N.; Nasri, M.; Ben Abdallah, F. (2016) Morphological and anatomical responses of pear and almond trees to fluoride air pollution. Fluoride , 49, 156–164.

Rouphael, Y., Cardarelli, M., Schwarz, D., Franken, P., & Colla, G. (2012). Effects of drought on nutrient uptake and assimilation in vegetable crops. In *Springer eBooks* (pp. 171–195). https://doi.org/10.1007/978-3-642-32653-0_7

Rudnick, R.L.; Gao, S. Composition of the continental crust. In Treatise on Geochemistry, 2nd ed.; Holland, H.D., Turekian, K.K., Eds.; Elsevier: Amsterdam, The Netherlands, 2014; Volume 4, pp. 1–51.

Saxena, V., & Ahmed, S. (2003). Inferring the chemical parameters for the dissolution of fluoride in groundwater. *Environmental Geology*, *43*(6), 731–736. https://doi.org/10.1007/s00254-002-0672-2

Segonzac, C., Boyer, J., Ipotesi, E., Szponarski, W., Tillard, P., Touraine, B., Sommerer, N., Rossignol, M., & Gibrat, R. (2007). Nitrate efflux at the root plasma membrane: identification of an arabidopsis excretion transporter. *The Plant Cell*, *19*(11), 3760–3777. https://doi.org/10.1105/tpc.106.048173

Serrano, M. J. G., Sanz, L. F. A., & Nordstrom, D. (2000). REE speciation in low-temperature acidic waters and the competitive effects of aluminum. *Chemical Geology*, *165*(3–4), 167–180. https://doi.org/10.1016/s0009-2541(99)00166-7

Shaji, E., Sarath, K., Santosh, M., Krishnaprasad, P., Arya, B., & Babu, M. S. (2023). Fluoride contamination in groundwater: A global review of the status, processes, challenges, and remedial measures. *Geoscience Frontiers*, *15*(2), 101734. https://doi.org/10.1016/j.gsf.2023.101734

Sharma, R., & Kaur, R. (2018). Insights into fluoride-induced oxidative stress and antioxidant defences in plants. Acta Physiologiae Plantarum, 40(10). https://doi.org/10.1007/s11738-018-2754-0

Singh, G.; Kumari, B.; Sinam, G.; Kumar, N.; Mallick, S. Fluoride distribution and contamination in the water, soil and plants continuum and its remedial technologies, an Indian perspective—A review. Environ. Pollut. 2018, 239, 95–108.

Singh, M.; Verma, K.K. (2013) Influence of fluoride-contaminated irrigation water on physiological responses of poplar seedlings (Populus deltoides clone-S7C15). Fluoride , 46, 83–89.

Skjelkvåle, B. L. (1994). Factors influencing fluoride concentrations in Norwegian lakes. *Water Air & Soil Pollution*, *77*(1–2), 151–167. https://doi.org/10.1007/bf00483055

Song, J., Hou, C., Guo, J., Niu, Q., Wang, X., Ren, Z., Zhang, Q., Feng, C., Liu, L., Tian, W., & Li, L. (2020). Two new members of CSFEXs couple proton gradients to export fluoride and participate in reducing fluoride accumulation in Low-Fluoride tea cultivars. *Journal of Agricultural and Food Chemistry*, *68*(32), 8568–8579. https://doi.org/10.1021/acs.jafc.0c03444

Stevens, D. P., McLaughlin, M. J., & Alston, A. M. (1997). Phytotoxicity of the fluoride ion and its uptake from solution culture by Avena sativa and Lycopersicon esculentum. *Plant and Soil*, *200*, 119–129.

Stockbridge, R. B., Kolmakova-Partensky, L., Shane, T., Koide, A., Koide, S., Miller, C., & Newstead, S. (2015). Crystal structures of a double-barrelled fluoride ion channel. *Nature*, *525*(7570), 548–551. https://doi.org/10.1038/nature14981

Stockbridge, R. B., Lim, H., Otten, R., Williams, C., Shane, T., Weinberg, Z., & Miller, C. (2012). Fluoride resistance and transport by riboswitch-controlled CLC antiporters. *Proceedings of the National Academy of Sciences*, *109*(38), 15289–15294. https://doi.org/10.1073/pnas.1210896109

Stockbridge, R. B., Robertson, J. L., Kolmakova-Partensky, L., & Miller, C. (2013). A family of fluoride-specific ion channels with dual-topology architecture. *eLife*, *2*, e01084. https://doi.org/10.7554/elife.01084

Streat, M., Hellgardt, K., & Newton, N. (2008). Hydrous ferric oxide as an adsorbent in water treatment. *Process Safety and Environmental Protection*, *86*(1), 21–30. https://doi.org/10.1016/j.psep.2007.10.009

Takeda, T., & Takizawa, S. (2008). Health risks of fluoride in the Chiang Mai Basin, Thailand. In *Library for sustainable urban regeneration* (pp. 301–327). https://doi.org/10.1007/978-4-431-78399-2_15

Tausta, S. L., Berbasova, T., Peverelli, M., & Strobel, S. A. (2021). The fluoride transporter FLUORIDE EXPORTER (FEX) is the major mechanism of tolerance to fluoride toxicity in plants1. *PLANT PHYSIOLOGY*, *186*(2), 1143–1158. https://doi.org/10.1093/plphys/kiab131

Tjahyono, N.; Gao, Y.; Wong, D.; Zhang, W.; Taylor, M.P. (2011). Fluoride emissions management guide (FEMG) for aluminium smelters. In Light Metals; Lindsay, S.J., Ed.; Springer: Cham, Switzerland, ; pp. 301–306.

Tsay, Y. (1993). The herbicide sensitivity gene CHL1 of arabidopsis encodes a nitrate-inducible nitrate transporter. *Cell*, *72*(5), 705–713. https://doi.org/10.1016/0092-8674(93)90399-b

Tsay, Y., Chiu, C., Tsai, C., Ho, C., & Hsu, P. (2007). Nitrate transporters and peptide transporters. *FEBS Letters*, *581*(12), 2290–2300. https://doi.org/10.1016/j.febslet.2007.04.047

Tylenda, C.A. (2011) Toxicological Profile for Fluorides, Hydrogen Fluoride, and Fluorine; DIANE Publishing: Collingdale, PA, USA, ; pp. 211–213.

Verma, K.K.; Verma, P.; Singh, M.; Verma, C.L. (2022) Influence of fluoride phytotoxicity in germinating seedlings of Pisum sativum: Modeling of morpho-physiological traits. Vegetos , 35, 736–746.

Vidal, E. A., Alvarez, J. M., Araus, V., Riveras, E., Brooks, M. D., Krouk, G., Ruffel, S., Lejay, L., Crawford, N. M., Coruzzi, G. M., & Gutiérrez, R. A. (2020). Nitrate in 2020: Thirty Years from Transport to Signaling Networks. *The Plant Cell*, *32*(7), 2094–2119. https://doi.org/10.1105/tpc.19.00748

Vithanage, M.; Bhattacharya, P. (2015) Fluoride in the environment: Sources, distribution and defluoridation. Environ. Chem. Lett. , 13, 131–147.

Von Der Fecht-Bartenbach, J., Bogner, M., Dynowski, M., & Ludewig, U. (2010). CLC-B-Mediated NOFormula/H+ exchange across the tonoplast of Arabidopsis vacuoles. *Plant and Cell Physiology*, *51*(6), 960–968. https://doi.org/10.1093/pcp/pcq062

Von Wittgenstein, N. J., Le, C. H., Hawkins, B. J., & Ehlting, J. (2014). Evolutionary classification of ammonium, nitrate, and peptide transporters in land plants. *BMC Evolutionary Biology*, *14*(1), 11. https://doi.org/10.1186/1471-2148-14-11

Wang, H., Yang, L., Gao, P., Deng, P., Yue, Y., Tian, L., Xie, J., Chen, M., Luo, Y., Liang, Y., Qing, W., Zhou, Z., Pi, H., & Yu, Z. (2022). Fluoride exposure induces lysosomal dysfunction unveiled by an integrated transcriptomic and metabolomic study in bone marrow mesenchymal stem cells. Ecotoxicology and Environmental Safety, 239, 113672.

Wang, J., Yu, X., Ding, Z. J., Zhang, X., Luo, Y., Xu, X., Xie, Y., Li, X., Yuan, T., Zheng, S. J., Yang, W., & Guo, J. (2021). Structural basis of ALMT1-mediated aluminum resistance in Arabidopsis. *Cell Research*, *32*(1), 89–98. https://doi.org/10.1038/s41422-021-00587-6

Wang, Y., Cheng, Y., Chen, K., & Tsay, Y. (2018). Nitrate transport, signaling, and use efficiency. *Annual Review of Plant Biology*, *69*(1), 85–122. https://doi.org/10.1146/annurev-arplant-042817-040056

Wang, Y., Huang, Y., Wang, J., Cheng, C., Huang, W., Lu, P., Xu, Y., Wang, P., Yan, N., & Shi, Y. (2009). Structure of the formate transporter FocA reveals a pentameric aquaporin-like channel. *Nature*, *462*(7272), 467–472. https://doi.org/10.1038/nature08610

Wen, Z., Tyerman, S. D., Dechorgnat, J., Ovchinnikova, E., Dhugga, K. S., & Kaiser, B. N. (2017). Maize NPF6 proteins are homologs of arabidopsis CHL1 that are selective for both nitrate and chloride. *The Plant Cell*, *29*(10), 2581–2596. https://doi.org/10.1105/tpc.16.00724

Wu, Y., Henderson, S. W., Walker, R. R., & Gilliham, M. (2022). Root-Specific Expression of Vitis vinifera VviNPF2.2 Modulates Shoot Anion Concentration in Transgenic Arabidopsis. *Frontiers in Plant Science*, *13*, 863971. https://doi.org/10.3389/fpls.2022.863971

Xiao, Q., Chen, Y., Liu, C., Robson, F., Roy, S., Cheng, X., Wen, J., Mysore, K., Miller, A. J., & Murray, J. D. (2021). MtNPF6.5 mediates chloride uptake and nitrate preference in Medicago roots. *The EMBO Journal*, *40*(21), e106847. https://doi.org/10.15252/embj.2020106847

Yang, J., Liu, C., Li, J., Zhang, Y., Zhu, C., Gu, D., & Zeng, L. (2024). Critical review of fluoride in tea plants (Camellia sinensis): absorption, transportation, tolerance mechanisms, and defluorination measures. *Beverage Plant Research*, *4*(1), 0. https://doi.org/10.48130/bpr-0024-0010

Zhang, J., Song, D., Schackert, F. K., Li, J., Xiang, S., Tian, C., Gong, W., Carloni, P., Alfonso-Prieto, M., & Shi, C. (2023). Fluoride permeation mechanism of the Fluc channel in liposomes revealed by solid-state NMR. *Science Advances*, *9*(34), eadg9709. https://doi.org/10.1126/sciadv.adg9709

Zhang, X., Bai, S., Min, H., Cui, Y., Sun, Y., & Feng, Y. (2025). Evolutionary dynamics of nitrate uptake, assimilation, and signalling in plants: adapting to a changing environment. Physiologia Plantarum, 177.

Zhao, S., Guo, J., Xue, H., Meng, J., Xie, D., Liu, X., Yu, Q., Zhong, H., & Jiang, P. (2022). Systematic impacts of fluoride exposure on the metabolomics of rats. Ecotoxicology and Environmental Safety, 242, 113888.

Zhou, G., Li, Q., Hou, X., Wu, H., Fu, X., Wang, G., Ma, J., Cheng, X., Yang, Y., Chen, R., Li, Z., Yu, F., Zhu, J., & Ba, Y. (2023). Integrated 16S rDNA sequencing and metabolomics to explore the intestinal changes in children and rats with dental fluorosis. Ecotoxicology and Environmental Safety, 251, 114518.

Zhu, J., Xing, A., Wu, Z., Tao, J., Ma, Y., Wen, B., Zhu, X., Fang, W., & Wang, Y. (2019). CsFEX, a Fluoride Export Protein Gene from Camellia sinensis, Alleviates Fluoride Toxicity in Transgenic Escherichia coli and Arabidopsis thaliana. *Journal of Agricultural and Food Chemistry*, *67*(21), 5997–6006. https://doi.org/10.1021/acs.jafc.9b00509

Zhu, M., Ding, K., Jiang, X., & Wang, H. (2007). Investigation on co-sorption and desorption of fluoride and phosphate in a red soil of China. *Water Air & Soil Pollution*, *183*(1–4), 455–465. https://doi.org/10.1007/s11270-007-9394-0

Zouari M, Elloumi N, Bellassoued K, Ahmed CB, Krayen M, Delmail D, Elfeki A, Rouina BB, Abdallh FB, Labrousse P (2017) Enzymatic antioxidant responses and mineral status in roots and leaves of olive plants subjected to fluoride stress. South Afr J Bot 111:44–49. https://doi.org/10.1016/j.sajb.2017.03.039